5-1970

Cation Exchange and Transport in Soil Columns Undergoing Miscible Displacement

Sung-ho Lai
Utah State University

Utah State University
MERRILL-CAZIER LIBRARY

CATION EXCHANGE AND TRANSPORT

IN SOIL COLUMNS UNDERGOING

MISCIBLE DISPLACEMENT

by

Sung-ho Lai

A dissertation submitted in partial fulfillment
of the requirements for the degree

of

DOCTOR OF PHILOSOPHY

in

Soil Science

Approved:

UTAH STATE UNIVERSITY
Logan, Utah

1970

ACKNOWLEDGMENTS

The conception of this dissertation began when I was studying at the University of California, Davis. I wish to extend my appreciation to Drs. J. W. Biggar and D. R. Nielsen for their help and encouragement during my stay at Davis.
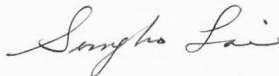
I wish to express my profound appreciation for the opportunity that Dr. J. J. Jurinak offered me to carry out this research and for the guidance and help he gave me toward the completion of this work.

I wish to thank Dr. R. J. Hanks for his generous assistance and constructive criticism toward the research and for his direction which ignited my interest in numerical mathematics. Thanks are also extended to Dr. J. D. Watson for his interest and guidance which helped me tremendously in the development of the mathematic solution of the problem.

Thanks are also offered to Dr. T. D. Alger and Dr. R. L. Smith for serving in my graduate committee and to Dr. K. T. Erh for providing me with the soils for this study.

Special thanks are extended to my wife, Sandra, for correcting and typing the manuscript and for her mental support during the last two years of my graduate study.

Sung-ho Lai

This work is dedicated to the memory
of my mother Yuh-Shiang Shieh Lai （賴謝玉香）

NOTATION

A: crossectional area (cm^2)

A: also general symbol for cation species

a_A, a_B: activity of cation A and B, respectively

B: general symbol for cation species

C: concentration in general (me/ml)

C_A, C_B, C_i: cation concentration for cation species A, B, and i, respectively (me/ml)

C_o: total cation concentration (me/ml)

c: a constant involved in exchange function

D: fluid dispersion coefficient (cm^2/hr)

f: functional symbol

f': derivative of the function f

f_A, f_B: activity coefficient of ion species A and B, respectively

F: functional symbol

g: functional symbol

i: general symbol for cation species

i: also the subscript for depth increment; usually appears along with j

j: subscript for time increment

K: equilibrium constant

K_B^A: selectivity coefficient

K', K'': constants involved in exchange function

k_1, k_2: rate constants

L: column length (cm)

N: subscript for the last depth increment where $z = L$

P_A, P_B: parameters related to the statistical thermodynamics properties of the cation species A and B

q_1: cation concentration per unit length of the exchanger phase (me/cm)

q: cation concentration per unit weight of exchanger (me/g)

q_A, q_B, q_i: cation concentration for cation species A, B, and i, respectively, per unit weight of the exchanger (me/g)

Q: cation exchange capacity per unit weight of the exchanger (me/g)

Q_1: cation exchange capacity per unit length of the exchanger

r: equilibrium parameter for ion exchange, $r = 1/K$

R: a symbol for cation exchanger

s: column-capacity parameter

S_o: slope of the breakthrough curve at $C/C_o = 0.5$

S_B^A: the separation factor

t: time (hr)

Δt: time increment

v: bulk volume of the column (cm^3)

V: volume of input solution or volume of the effluent solution at time t (ml)

V_o: pore volume or effluent volume when $C/C_o = 0.5$ (ml)

$\bar{V}$: average interstitial flow velocity (cm/hr)

X_A, X_B, X_i: relative concentration for cation species A, B, and i, respectively, in solution (dimensionless)

X: relative concentration of cation in solution in general

X^n: relative concentration of the nth iteration

$X(z,t)$: relative cation concentration function in the solution phase

Y_A, Y_B, Y_i: relative concentration of cation in the exchanger phase for cation species A, B, and i, respectively

Y: relative concentration of cation in the exchanger phase in general

$Y(z,t)$: relative concentration function of the exchanger phase

z: depth of the column (cm)

Δz: depth increment (cm)

α: pore fraction

ε: tolerance limit, a very small value

ψ: function symbol

θ: function symbol

ϕ: function symbol

λ: concentration ratio parameter

ρ: bulk density (g/cm^3)

$\gamma_A, \gamma_B, \gamma_i$: valency of the cation species A, B, and i, respectively

τ: solution-capacity parameter

ω: concentration ratio parameter for the exchanger phase

TABLE OF CONTENTS

TABLE OF CONTENTS (Continued)

TABLE OF CONTENTS (Continued)

LIST OF TABLES

LIST OF TABLES (Continued)

LIST OF FIGURES

LIST OF FIGURES (Continued)

LIST OF FIGURES (Continued)

ABSTRACT

Cation Exchange and Transport

in Soil Columns Undergoing

Miscible Displacement

by

Sung-ho Lai, Doctor of Philosophy

Utah State University, 1970

Major Professor: Dr. J. J. Jurinak
Department: Soils and Meteorology

A mathematical model was developed to predict the exchange of one cation by another in a soil column undergoing one dimensional cation solution displacement under steady state flow conditions. The model allowed prediction of both the solution and exchanger phase concentration of the cation in question.

The model consists of a material balance equation which is a parabolic type partial differential equation. The assumption was made that equilibrium was reached instantaneously between the cations in the solution phase and the exchanger phase. This assumption reduced the material balance equation to a form that allowed numerical solution providing the data concerning the cation exchange isotherm and the initial and boundary conditions are available.

FORTRAN programs were written for the numerical computation of the problem involved. The computation was done on a digital computer.

The model was verified by comparing the theoretically computed cation concentration profile with data from actual soil column experiments.

The cation exchange of $Mg \rightarrow Ca$ was tested on Yolo fine sandy loam, Nibley clay loam and Hanford sandy loam columns. The exchange of $Na \rightarrow Ca$ was also tested on Yolo fine sandy loam. Satisfactory agreement between the column experiment values and the theoretically computed values was obtained.

(144 pages)

INTRODUCTION

Background

The transport of chemical identities through a soil body is a subject of concern not only to the agriculturalist and environmental scientist, but also to the people in the fields of water quality, civil engineering, and chemistry.

This writer is particularly interested in the study of one dimensional transport of cations through an isotropic soil column during the miscible displacement of two different cation solutions in a steady flow condition. This subject was first studied by Rible and Davis (1955) and then by Bower et al. (1957). Both studies ignore the effect of fluid dispersion which was shown to be operative to a significant extent by Lapidus and Amundson (1952). The model proposed by Lapidus and Amundson was applicable to a certain extent in the cation transport in soil. Their study was limited to the cation exchange or adsorption processes which had a linear isotherm or a linear kinetics of cation exchange or adsorption. Since a great deal of evidence suggests that the cation exchange isotherm in soils is non-linear, a non-linear approach is necessary to deal with the problem. Fortunately, with the great invention of digital computers and their widespread use in recent years, numerical mathematics has been revived and is advancing at a very fast pace. Now, there are methods to handle the model that was proposed by Lapidus and Amundson involving a non-linear isotherm.

Objectives

It is the objective of this study to modify the model that was proposed by Lapidus and Amundson and to solve it numerically for the cation exchange reaction that occurs in a soil system; and to investigate the effect of different types of exchange isotherms on cation transport processes. The theoretical solution is then verified by conducting column experiments under specified conditions.

This type of study gives insight into how different types of exchange reactions influence the transport of cations through a soil column, how the cation composition of the fluid and the soil exchanger changes through the soil body. This information is useful in many phases of agriculture including irrigation, land drainage, water quality, and waste disposal management. This study also offers a broader perspective toward the study of the transport of the other types of chemical identities such as anion transport and transport of organic and inorganic molecules through an adsorbent bed. All of these subjects are so vital to the conservation of the quality of the environment that it merits thorough investigation.

Definitions

The *exchanging cation* is the cation in solution which exchanges with the cation which was adsorbed by the cation exchanger. The *cation exchanger* is the solid material which possesses the net negative electric charge which adsorbs cations.

The *exchange isotherm* shows the ionic composition of the cation exchanger as a function of the ionic composition of the solution at

equilibrium and at constant temperature. In this study, the equivalent ionic fraction Y_A of the exchanging ion A in the cation exchanger is plotted as a function of the equivalent fraction X_A in the solution. The *equivalent ionic fraction* in solution is defined by

$$X_A = \frac{C_A}{\Sigma C_i} \qquad [1]$$

where C_A is the concentration of the cation A in terms of me/l in solution. The equivalent fraction in the exchanger phase is defined by

$$Y_A = \frac{q_A}{\Sigma q_i} \qquad [2]$$

where q_i is expressed in me per gram of the exchanger.

The *exchange function* is the functional relation which expresses Y_A in terms of X_A. This term is sometimes used interchangeably with the term *exchange isotherm*.

A *concentration profile* expresses the concentration of the cation as a function of depth usually at a given time. It can be for the solution phase $X(x,t)$ or for the exchanger phase $Y(z,t)$, both expressed at a given time t.

The *separation factor* expresses the preference of the ion exchanger for one of the two counter ions. It is written as

$$S_B^A = \frac{Y_A X_B}{Y_B X_A} \qquad [3]$$

If the ion A is preferred, the factor S_B^A is larger than unity.

The rational *selectivity coefficient* is defined as

$$K_B^A = \frac{Y_A^{\gamma_B} X_B^{\gamma_A}}{Y_B^{\gamma_A} X_A^{\gamma_B}}$$

[4]

The essential difference between the separation factor and the selectivity coefficient is that the latter contains the ionic valances as exponents. It can be considered as the uncorrected equilibrium constant.

LITERATURE REVIEW

Ion Exchange Chromatography

The foundation of ion exchange cromatography is based on the con-
cepts of material conservation. That is to say, the change in the
material flux within a section of column Δz is equal to the sum of the
rate of change in the concentration of the solution phase and the rate
of change in the concentration of the exchanger phase within the sec-
tion.

Two different approaches can be identified in the literature
according to the treatment of the rate of ion exchange. The one that
was developed by Thomas (1944) was based on a second order kinetics.
The second one developed by DeVault (1943) was based on the assumption
that an instantaneous equilibrium between solution phase and exchange
phase exists. The historical development of these two different schools
will be reviewed separately in the following sections. An additional
model which includes the fluid dispersion effect will also be reviewed.

Kinetic approach

The model developed by Thomas (1944) was based on the condition
of the conservation of the exchanging ions. It required that within
a finite section of the column, the change in solute flux must be
accounted for by the rate of change of the solution concentration and
the rate of change of the concentration of the exchanger phase. This

is more vividly depicted by Equation [5] which is written in terms of
the notation defined in this paper

$$\bar{V} \frac{\partial C}{\partial z} + \frac{\partial C}{\partial t} + \frac{\rho}{\alpha} \frac{\partial q}{\partial t} = 0 \qquad [5]$$

where C is the concentration of the cation in solution, q is the amount
of cation adsorbed per unit weight of the adsorbent, z is the depth of
the column, t is time, $\bar{V}$ is the interstitial flow velocity, ρ is the bulk
density of the soil column and α is the pore fraction of the column. The
characteristic of Thomas' study is the treatment of the reaction rate of
the cation exchange. A second order reaction kinetic was used for a
univalent cation exchange reaction on zeolite such as

$$A^+ + BR \rightarrow AR + B^+ \qquad [6]$$

$$\frac{\partial q}{\partial t} = k_1 C(Q - q) - k_2 q(C_o - C) \qquad [7]$$

where A and B are cations R is the exchanger, Q is the cation exchange
capacity, C_o is the total concentration of the cations, and k_1 and k_2
are the rate constants.
Equations [5] and [7] were solved by providing the initial and the boun-
dary conditions.

This approach was further extended by Hiester and Vermeulen (1952)
by rewriting Equation [5] as

$$- \left(\frac{\partial C}{\partial v}\right)_V = \rho \left(\frac{\partial q}{\partial v}\right)_V + \alpha \left(\frac{\partial C}{\partial v}\right)_V \qquad [8]$$

and by slightly modifying the kinetic Equation [7] to

$$\left(\frac{\partial q}{\partial t}\right) = k_1 [C(Q - q) - \frac{1}{K} q(C_o - C)] \qquad [9]$$

where v is the bulk volume of the column, V is the volume of the input solution and $K = \frac{k_1}{k_2}$. They further defined a solution capacity parameter τ, a column capacity parameter s, and the equilibrium parameter r, to reduce Equation [8] to

$$- \left(\frac{\partial (q/Q)}{\partial \tau}\right)_s = \left(\frac{\partial (C/C_0)}{\partial s}\right)_\tau \qquad [10]$$

and Equation [9] to

$$\left(\frac{\partial (q/Q)}{\partial \tau}\right)_s = C/C_o(1 - q/Q) - rq/Q(1 - C/C_o) \qquad [11]$$

The solutions C/C_o and q/Q were obtained by a numerical curve matching method referring to the three parameters τ, s, and r. This paper by Hiester and Vermeulen is recognized as one of the classic treatments in the field of chromatography. It also includes the study of chromatography involving physical adsorption. For further details, this paper should be consulted.

Application of this model in the field of soil science was done by Bower, Gardner, and Goertzen (1957). Their work is essentially a test of the validity of the Hiester-Vermeulen approach to the cation exchange reaction in soil columns. They further define two parameters namely λ, the concentration ratio parameter for the solution, and ω, the concentration ratio parameter for the exchanger phase. Equations [10] and [11] were reduced to

$$\left(\frac{\partial \omega}{\partial \tau}\right)_s = \left(\frac{\partial \lambda}{\partial s}\right)_\tau \qquad [12]$$

$$\left(\frac{\partial \omega}{\partial \tau}\right)_s = \lambda(1 - \omega) - r\omega(1 - \lambda) \qquad [13]$$

The solution of these equations was provided graphically by Hiester and Vermeulen (1952). The experimental results were in good agreement with the theoretical prediction in this particular study.

Equilibrium approach

The model developed by DeVault (1943) for single solute chromatography was also based on the same conditions of solute conservation in the column process and is described by an equation similar to that of Equation [5]

$$\frac{\partial C}{\partial z} + \alpha \frac{\partial C}{\partial V} + \frac{\partial q_1}{\partial V} = 0 \qquad [14]$$

where q_1 is the cation adsorbed per unit length of the exchanger. The characteristic of this model is that DeVault assumed an instantaneous equilibrium between the solute in solution and that in the exchanger. The equilibrium relationship between the solute exchanged and solute in solution is defined as an isotherm and is expressed as a function of concentration $f = f(C)$ and $f(C) = q_1/Q_1$, where Q_1 is the cation exchange capacity per unit length of the exchanger. Thus, the rate of exchange is now a function of the rate of solution concentration change and the slope of the exchange isotherm

$$\frac{\partial^q 1}{\partial V} = Q_1 \frac{\partial f(C)}{\partial V} = Q_1 \left[\frac{df}{dC}\right]\frac{\partial C}{\partial V} \qquad [15]$$

Equation [14] is simplified to

$$\frac{\partial C}{\partial z} + [\alpha + Q_1 f'(C)]\frac{\partial C}{\partial V} = 0 \qquad [16]$$

This equation is further simplified to

$$\left(\frac{\partial V}{\partial z}\right)_C = \alpha + Q_1 f'(C) \qquad [17]$$

and with

$$(z)_{V = 0} = F(C)$$

the solution of z as a function of C and V is

$$z = F(C) + \frac{V}{\alpha + Q_1 f'(C)} \qquad [18]$$

This approach is mathematically less involved. The applicability of this model was tested for soil system by Rible and Davis (1955) with a certain degree of success. However, critical examination of their experimental results indicated a decided tendency for the concentration profiles to spread whereas the theoretical model predicts a sharp profile.

Dispersion and chromatography

Neither the kinetic nor the equilibrium approaches of the previous section considered the fluid dispersion effect. Fluid dispersion is

another factor that can cause the spreading of the fluid from the idealized piston flow in a column. Lapidus and Amundson (1952) developed a model which takes into account the dispersion in addition to the mass flow in the flux term of the material balance equation. The equation is written as

$$D \frac{\partial^2 C}{\partial z^2} = \bar{V} \frac{\partial C}{\partial z} + \frac{\partial C}{\partial t} + \frac{\rho}{\alpha} \frac{\partial q}{\partial t} \qquad [19]$$

where D is the fluid dispersion coefficient. They treated the rate of exchange or adsorption in two separate cases. One of the cases involved instantaneous equilibrium. Thus,

$$q = k_1 C + k_2 \qquad [20]$$

In another case, they used a linear kinetics approach to describe the rate of exchange or adsorption

$$\frac{\partial q}{\partial t} = k_1 C - k_2 q \qquad [21]$$

In both cases, the solution was obtained analytically and are mathematically complicated, involving functions which are usually tabulated in a mathematical handbook.

The analytical solution of Equations [19] and [21] was also obtained by Ogata (1964) using the Laplace transformation. The work was purely mathematical and its applicability was not tested experimentally.

A comparative study of the three models, DeVault's equilibrium model, Thomas-Hiester and Vermeulen's kinetic model, and the Lapidus and Amundson's model was reported by Bigger and Nielsen (1963) using Oakley sand. According to their report, none of these models strictly agree with the experimental value. The lack of agreement was attributed to factors such as inadequate description of exchange, the use of the average value for the flow velocity, and the dispersion coefficient. It was concluded that the Lapidus and Amundson model was qualitatively the best model of the three in predicting experimental data.

Ion Exchange Equilibrium in Soil

In treating ion exchange equilibria of zeolite, Helfferich (1962) classified the exchange equilibria into two groups depending on the behavior of the exchange isotherm it possesses. The two groups are the "regular" system and the "irregular" system. These two groups of the exchange equilibria will be reviewed, since it appears to be a reasonable approach to exchange equilibria.

"Regular" system

The "regular" system includes the exchange reaction which shows a constant selectivity coefficient. The early development of the theory of cation exchange in soil science was based mainly on the mass action approach such as that of Vanselow and Gapon as cited by Babcock (1963). For the exchange reaction

$$\gamma_B A_{(ad)} + \gamma_A B \rightleftarrows \gamma_B A + \gamma_A B_{(ad)} \qquad [22]$$
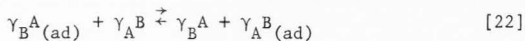
with γ_A and γ_B representing the valancy of cation A and B, respectively. The equilibrium is expressed as

$$\frac{q_B^{\gamma_A} c_A^{\gamma_B}}{q_A^{\gamma_B} c_B^{\gamma_A}} = K_A^B \qquad [23]$$

where the selectivity coefficient K_A^B is a constant. This type of approach follows the thermodynamics reasoning of chemical equilibrium and is applicable mainly to a homogenous solid exchanger.

Clark and Turner (1965) used the equivalent fraction for both the solution phase and the exchanger phase and obtained the following expression

$$\frac{(1 - Y_A)^{\gamma_A}}{Y_A^{\gamma_B}} \frac{X_A^{\gamma_B}}{(1 - X_A)^{\gamma_A} c_o^{\gamma_B - \gamma_A}} = K \frac{f_B^{\gamma_A}}{f_A^{\gamma_B}} \qquad [24]$$

where f_A and f_B are the activity coefficient for cation A and B, respectively. This expression includes the total ionic concentration of the solution C_o in the selectivity coefficient when it involves heterovalent exchange. The activity coefficient was evaluated by using the limiting law of Debye-Hückel when the total ionic concentration was dilute.

"Irregular" system

The "irregular" system includes all the cation exchange reactions that show a non-constant selectivity coefficient. Throughout the

historical development of the theory of cation exchange equilibria, ex-
perimental results have indicated that the selectivity coefficient may
not always be constant. Research has been directed toward the theoreti-
cal interpretation of the non-constant selectivity coefficient.
Krishnamoorthy and Overstreet (1949) applied a statistical thermodynamic
approach to derive an equation which describes the non-constant selecti-
vity coefficient for heterovalent reactions as shown in Equation [25].

$$\frac{(q_A)^{\gamma_B}}{(q_B)^{\gamma_A}} \; (p_A q_A + p_B q_B)^{\gamma_B} - \gamma_A \; \frac{(a_B)^{\gamma_A}}{(a_A)^{\gamma_B}} = K \qquad [25]$$

where p_A and p_B are the parameters depending on the valency of the ions.
The value of p_i equals 1, 1 1/2, and 2 for mono-valent, divalent, and
trivalent ions, respectively, and a_A, a_B are the activity of cations
A and B, respectively. Eriksson (1952) introduced the concept of charge
volume of the exchanger phase and arrived at Equation [26] which is very
similar to the one by Krishnamoorthy and Overstreet for Na^+ *vs* Ca^{++} ex-
change.

$$\frac{(q_{Na})^2 (C_{Ca}) Q}{(q_{Ca}) (C_{Na})^2 (q_{Na} + 2\,q_{Ca})} = K \qquad [26]$$

Both Equations [25] and [26] depict the possible non-constant selec-
tivity for heterovalent exchange. However, evidence of non-constant
selectivity for homovalent exchange required further theoretical
development. Barrer and Falconer (1956) interpretated the irregular

behavior of the homovalent exchange as a result from the fact that the occupancy of an exchange site by an A or B ion affects the relative affinities of the adjacent sites for these ions. They were able to give a more fundamental interpretation to the equation which was obtained by Kielland semi-empirically. The equation is written as

$$\ln \frac{a_B^{Y_A}}{a_A^{Y_B}} = \ln K + c(1 - 2Y_B) \qquad [27]$$

in which K is the rational equilibrium constant as defined by Helfferich (1962) and c is a constant. This equation is applicable for both the "irregular" and the "regular" systems. For a "regular" system, c = 0. For an "irregular" system, c ≠ 0. A more detailed description of this approach can be found in Helfferich (1962).

To use any of the derived exchange isotherms presented above, they must be presented in the form Y = f(X) in order to be used in the solution of the material balance equation. This will be described in the section entitled theoretical development.

THEORETICAL DEVELOPMENT

Mathematical Treatment

Derivation of the material
balance equation

The material balance equation discussed in the literature review appeared in several forms that were derived essentially by using the concept of mass conservation. The equation will be derived here, based on the one dimensional model in the hope that its derivation will give a better insight and understanding of the problem at hand.

A finite section of a packed soil column, which had a steady one dimensional flow established, was taken between z and $z + \Delta z$ as shown in Figure 1. According to the mass conservation concept, the difference in the flux of cations across the area at z and that at $z + \Delta z$ should be equal to the rate of change of the cation concentration in the solution phase plus the rate of change of the cation concentration in the adsorbed phase within this particular section of the soil. Thus, we can establish a balance formula such as

$$\begin{pmatrix} \text{net change} \\ \text{of ion flux} \end{pmatrix} = \begin{pmatrix} \text{rate of change} \\ \text{of} \\ \text{solution conc.} \end{pmatrix} + \begin{pmatrix} \text{rate of cation} \\ \text{exchange} \end{pmatrix} \qquad [28]$$

In the flow system, the flux consists of the transport due to the mass fluid flow and the fluid dispersion or

$$\text{Flux} = - D \frac{\partial C_i}{\partial z} + \bar{V} C_i \qquad [29]$$
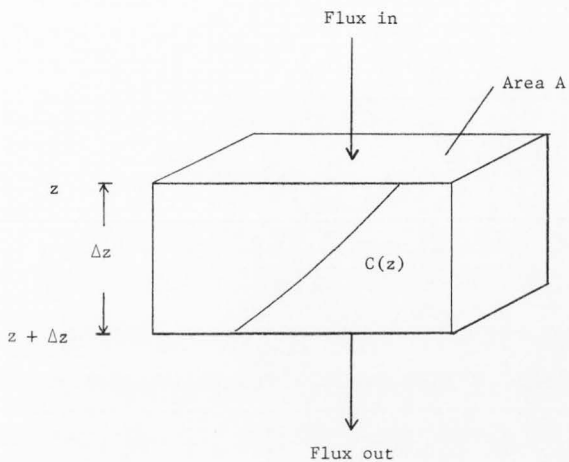
Figure 1. A schematic representation of the one-dimensional miscible displacement flow for a finite section of the column.

The two rate terms are defined as

$$\frac{\partial C_i}{\partial t} = \text{rate of change of } C_i$$

$$\frac{\partial q_i}{\partial t} = \text{rate of change of } q_i$$

Equation [28] is now written as

$$(A \cdot \alpha)[(- D \frac{\partial C_i}{\partial z} + \bar{V}C_i)_z - (- D \frac{\partial C_i}{\partial z} + \bar{V}C_i)_{z + \Delta z}] =$$

$$(A \cdot \alpha \cdot \Delta z) \frac{\partial C_i}{\partial t} + (A \cdot \Delta z \cdot \rho) \frac{\partial q_i}{\partial t} \qquad [30]$$

Dividing both sides by $(A \cdot \Delta z \cdot \alpha)$, we have

$$\frac{(D \frac{\partial C_i}{\partial z} - \bar{V}C_i)_{z + \Delta z} - (D \frac{\partial C_i}{\partial z} - \bar{V}C_i)_z}{\Delta z} = \frac{\partial C_i}{\partial t} + \frac{\rho}{\partial} \frac{\partial q_i}{\partial t} \qquad [31]$$

Since the left hand side of Equation [31] is the partial derivative of flux with respect to z, we have

$$\frac{\partial}{\partial z} (D \frac{\partial C_i}{\partial z} - \bar{V}C_i) = \frac{\partial C_i}{\partial t} + \frac{\rho}{\alpha} \frac{\partial q_i}{\partial t} \qquad [32]$$

For constant D and $\bar{V}$, Equation [32] can be further reduced to

$$D \frac{\partial^2 C_i}{\partial z^2} - \bar{V} \frac{\partial C_i}{\partial z} = \frac{\partial C_i}{\partial t} - \frac{\rho}{\alpha} \frac{\partial q_i}{\partial t} \qquad [33]$$

Equation [33] is similar to the material balance equation used by Lapidus and Amundson (Equation [19]).

Transformation of Equation [33]
to a working equation

Equation [33] is not immediately applicable to the method that will be used later in this study. It is desirable to transform this equation into a form such that the dependent variables reduced to dimensionless values and vary between 0.0 and 1.0. For a cation exchange reaction taking place in a constant total concentration, this is done easily by setting

$$C_o = C_A + C_B$$
$$Q = q_A + q_B$$

[34]

and defining X_i and Y_i so that

$$C_i = C_o X_i$$
$$q_i = QY_i$$

[35]

For the cation exchange reaction of constant total concentration in solution and a constant exchange capacity, C_o and Q are constant. We can obtain the following partial differential forms

$$\frac{\partial C_i}{\partial t} = C_o \frac{\partial X_i}{\partial t}$$

$$\frac{\partial C_i}{\partial z} = C_o \frac{\partial X_i}{\partial z}$$

$$\frac{\partial^2 C_i}{\partial z^2} = C_o \frac{\partial^2 X_i}{\partial z^2}$$

$$\frac{\partial q_i}{\partial t} = Q \frac{\partial Y_i}{\partial t}$$

[36]

Substituting Equation [36] into Equation [33], we obtain a reduced form of the material balance equation

$$D \frac{\partial^2 X_i}{\partial z^2} - \bar{V} \frac{\partial X_i}{\partial z} = \frac{\partial X_i}{\partial t} + \frac{\rho Q}{\alpha C_o} \frac{\partial Y_i}{\partial t} \qquad [37]$$

The assumption is made that an instantaneous equilibrium exists between the solution phase and the exchanger phase. If this assumption is true, we have a unique function that relates X_i and Y_i which is called an exchange isotherm or exchange function such as

$$Y_i = f(X_i) \qquad [38]$$

By using the chain rule, we can write

$$\frac{\partial Y_i}{\partial t} = \frac{df(X_i)}{dX_i} \frac{\partial X_i}{\partial t}$$

or $\qquad\qquad\qquad\qquad\qquad\qquad\qquad\qquad\qquad\qquad$ [39]

$$\frac{\partial Y_i}{\partial t} = f' \frac{\partial X_i}{\partial t}$$

where f' is the slope of the exchange isotherm. Substituting Equation [39] into Equation [37] and dropping the subscript i understanding that we are dealing with the exchanging ion, we have a simplified equation

$$D \frac{\partial^2 X}{\partial z^2} - \bar{V} \frac{\partial X}{\partial z} = (1 + \frac{\rho Q}{\alpha C_o} f') \frac{\partial X}{\partial t} \qquad [40]$$

Equation [40] can be solved numerically regardless of the form of $f(X)$, provided $f(X)$ is known and the initial condition and the boundary conditions are given.

The initial condition and
the boundary conditions

The initial condition. The initial condition involved in this
problem could be either a uniform or a non-uniform one. Thus, the
initial condition could be

$$X(z,0) = \psi(z) \qquad [41]$$

where ψ is either a constant or a function of z. In the cation dis-
placement experiment, the column is saturated with one kind of cation.
Thus, at the initial time, the column is without the exchanging cation.
In this case, we have $\psi = 0$ as the initial condition. Information
about $Y(z,0)$ is not necessary at this time because the equilibrium
relation relates Y to X.

The boundary conditions. The top boundary in this study is a
Dirichlet type as referred by Berg and McGregor (1966). It is ex-
pressed as

$$X(0,t) = \theta(t) \qquad [42]$$

Here $\theta(t)$ can either be a function of time or a constant. In this
study, we maintained the top boundary with pure exchanging cation
throughout the experiment. Thus, $\theta = 1.0$.

The bottom boundary is the Neumann type which is expressed as

$$\frac{\partial X(L,t)}{\partial z} = \phi(t) \qquad [43]$$

Here again the ϕ can either be a function of time or a constant. For
the cation displacement column study, the concentration gradient at

the effluent end was set to zero. Thus, $\phi = 0$. This type of treatment was proposed and discussed by Danckwerts (1953) and Brenner (1962).

Cation exchange function

The cation exchange function expresses Y as a function of X. This is graphically shown by the cation exchange isotherm plotted in terms of Y and X (see Figure 2).

In general, the equations of the cation exchange equilibria that were cited in the literature review section involve terms that are raised to the power of the valency of the cation concerned. This makes it rather complicated to arrive at an equation which will explicitly express Y in terms of X. Some of the exchange equations also contain the activity coefficients which cannot be calculated accurately in the concentration range used in this study.

In this study, we are not overly concerned about the theoretical interpretation of the cation exchange equilibria. Of major interest is finding a functional expression of Y in terms of X. This can be done by either using the experimental data to fit a regression equation or by finding out the functional relationship between the separation factor S_B^A and the concentration X and then arriving at an explicit expression of Y in terms of X.

It has been pointed out by Helfferich (1962) that the separation factor is a convenient quantity for the practical application of cation exchange such as the evaluation of the exchange column performance.
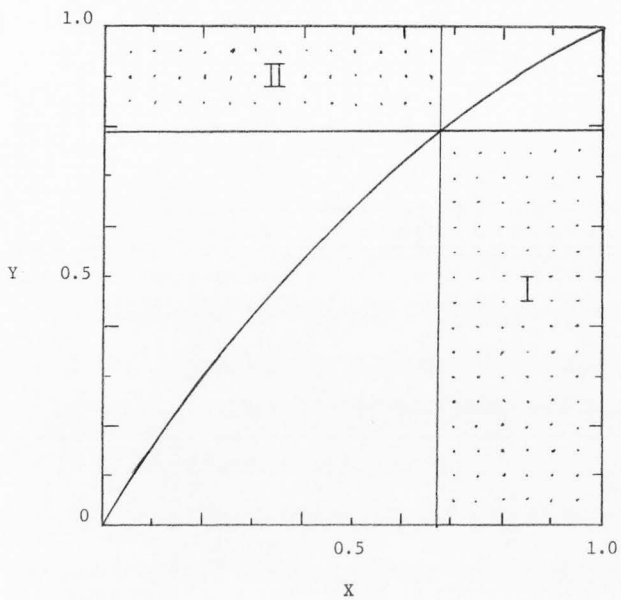
Figure 2. A diagram showing the relationship between the exchange
isotherm and the separation factor. The separation
factor S_B^A is represented by the ratio of areas I and II

The physical significance of the separation factor is that it represents the preference of the ion exchanger for one of the two counter ions. For $S_B^A > 1$, the exchanger prefers ion A, while for $S_B^A < 1$, the exchanger prefers ion B. For $S_B^A = 1$, the exchanger has no preference for either ion.

A schematic representation of the relationship between the separation factor and the exchange isotherm was adopted from Helfferich and is shown in Figure 2. In this diagram, the separation factor for any ionic composition equals the ratio of the two rectangular areas I and II which touch one another at the corresponding point on the isotherm.

The exchange function of the cation exchange reaction that shows a constant separation factor with respect to the ionic composition can be derived readily. Take the following example

$$A^+ + BR = AR + B^+ \tag{6}$$
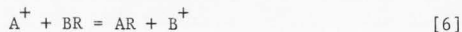
the separation factor is expressed as

$$\frac{Y_A X_B}{Y_B X_A} = S_B^A \tag{3}$$

Replacing X_B and Y_B by $(1 - X_A)$ and $(1 - Y_A)$, respectively, we obtain an expression of Y_A in terms of X_A such as

$$Y_A = \frac{X_A}{X_A + (1 - X_A)K'} \tag{44}$$

where K' equals $1/S_B^A$.

For the cation exchange of Na$\rightarrow$Ca in Yolo fine sandy loam soil, Equation [44] slightly deviated from the actual value measured. A modification was used such that

$$Y_A = \frac{X_A}{X_A + (1 - X_A)[K'' + c(1 - 2X_A)]} \qquad [45]$$

This equation is based on the premise that the separation factor is a function of the ionic composition of the solution such as

$$S_B^A = \frac{1}{K'' + c(1 - 2X_A)} \qquad [46]$$

The applicability of this approach is tested in the experiment.

Another type of exchange function that is used in this study also involves a variable separation factor. The derivation of this function is based on Equation [27]. Equation [27] is now written in a slightly different form so that the Y_B on the right hand side is replaced by X_B.

$$\ln \frac{Y_A X_B}{Y_B X_A} = \ln K + c(1 - 2X_B) \qquad [47]$$

where K includes both the rational thermodynamic equilibrium constant and the ratio of the activity coefficient f_A/f_B. By replacing X_A and Y_A by $(1 - X_B)$ and $(1 - Y_B)$, respectively, and by rearranging the terms, we obtain the exchange function

$$Y_B = \frac{X_B}{X_B + (1 - X_B) \, \mathrm{Exp}[\ln K + c(1 - 2X_B)]} \qquad [48]$$

The similarity of Equation [45] to Equation [48] is easily seen. The applicability of Equation [48] will be discussed later.

Longitudinal dispersion

The spreading of a solute due to dispersion in the fluid moving through a porous media can be described by the equation

$$\frac{\partial C}{\partial t} = -\bar{V}\frac{\partial C}{\partial z} + D\frac{\partial^2 C}{\partial z^2}$$ [49]

The solution of this equation was written by Rifai, Kaufman, and Todd (1956) as

$$\frac{C}{C_o} = \frac{1}{2}\left(1 \pm \text{erf}\ \frac{z - \bar{V}t}{2\sqrt{Dt}}\right)$$ [50]

where the sign is "+" for $z<\bar{V}t$ and "−" for $z>\bar{V}t$.

The dispersion coefficient is calculated from Equation [50] by knowing the value of C/C_o on a breakthrough curve of a non-reacting solute when $z = L$.

An improved method of calculating D was developed by Rifai et al. They differentiated Equation [50] with respect to the effluent volume V and defined S_o as :

$$S_o = \frac{d(C/C_o)}{dV}\ \bigg|\ V = V_o$$

This resulted in the equation

$$\frac{D}{\bar{V}} = \frac{L}{4\pi V_o^2 S_o^2}$$ [51]

where V_o is the effluent volume at $C/C_o = 0.5$ and S_o is the slope of the breakthrough curve at $C/C_o = 0.5$. The details of the derivation of Equation [51] from Equation [50] are shown in Appendix B.

Numerical Solution and Computation

The equations which require mathematical solution are Equation [40] through Equation [43]. They are summarized below:

$$D \frac{\partial^2 X}{\partial z^2} - \bar{V} \frac{\partial X}{\partial z} = (1 + \frac{\rho Q}{\alpha C_o} f') \frac{\partial X}{\partial t} \qquad [40]$$

$$X(z,0) = 0 \qquad [41]$$

$$X(0,t) = 1.0 \qquad [42]$$

$$\frac{\partial X(L,t)}{\partial z} = 0 \qquad [43]$$

where $f' = \frac{df}{dX}$.

The partial differential equation (PDE) can be solved numerically by the explicit method or by the implicit method, both outlined by Ames (1965) and Carnahan, Luther, and Wilkes (1969). In this study, the explicit method and the implicit method were both used and compared.

The explicit method

The finite difference schemes for the PDE are as follows:

$$\frac{\partial X}{\partial t} \simeq \frac{X_{i,j+1} - X_{i,j}}{\Delta t}$$

$$\frac{\partial^2 X}{\partial z^2} \simeq \frac{X_{i+1,j} - 2X_{i,j} + X_{i-1,j}}{\Delta z^2} \qquad [52]$$

$$\frac{\partial X}{\partial z} \simeq \frac{X_{i+1,j} - X_{i-1,j}}{2\Delta z}$$

where i is now a subscript for the depth increment and j is a subscript for the time increment. Since f' is a function of X alone, we let

$$g(X) = (1 + \frac{\rho Q}{\alpha C_o} f'(X))$$

$$g(X) \simeq g(X_{i,j})$$

[53]

Substituting Equations [52] and [53] into Equation [40], and rearranging the terms, we obtain

$$X_{i,j+1} = \frac{\Delta t}{g(X_{i,j})} [(\frac{D}{\Delta z^2} - \frac{\bar{V}}{2\Delta z}) X_{i+1,j} - (\frac{2D}{\Delta z^2} - \frac{g(X_{i,j})}{\Delta t}) X_{i,j} +$$

$$(\frac{D}{\Delta z^2} + \frac{\bar{V}}{2\Delta z}) X_{i-1,j}]$$

[54]

The initial condition is

$$X_{i,0} = 0$$

The boundary conditions are

$$X_{0,j} = 1.0$$

$$\frac{X_{N+1,j} - X_{N-1,j}}{2\Delta z} = 0$$

[55]

or

$$X_{N+1,j} = X_{N-1,j}$$

where N is the subscript for the last depth increment. A grid network is constructed to represent the problem in the z and t coordinates (see Figure 3a). The computation scheme represented by
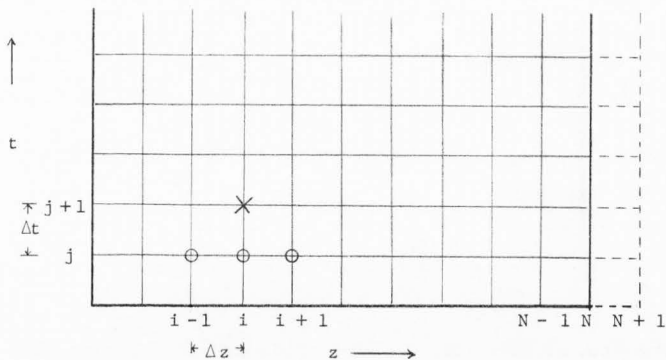
Figure 3a. A grid network showing the relationship of the four finite
elements of Equation [54]. The three elements encircled
are known. The value in the cross is evaluated by the
three in the circles.
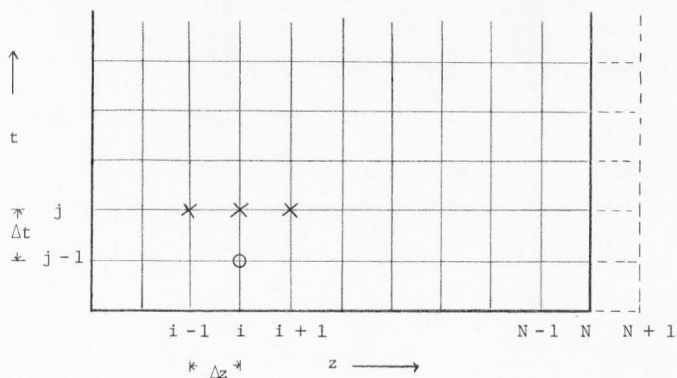
Figure 3b. A grid network showing the relationship of the four finite
elements of Equation [57]. The three elements in the
crosses are evaluated by the one in the circle.

Equation [54] is also presented in Figure 3a. The computation of $X_{i,j + 1}$ involves values of $X_{i - 1,j}$, $X_{i,j}$, and $X_{i + 1,j}$. After every value of X in the j + 1 row is computed, this row becomes the initial value for the calculation of X in the next row. The computation continues until the values of X of the desired time increment are computed.

In order to have a stable and converged solution from this method, it is necessary to set the depth increment Δz and the time increment Δt so that

$$0 < \frac{\Delta t}{(\Delta z)^2} \leq \frac{1}{2}$$

The implicit method
(predictor-corrector technique)

The finite difference schemes for the implicit method used in this study are slightly different from those used for the explicit method. They are listed as follows:

$$\frac{\partial X}{\partial t} \simeq \frac{X_{i,j} - X_{i,j - 1}}{\Delta t}$$

$$\frac{\partial^2 X}{\partial z^2} \simeq \frac{X_{i + 1,j} - 2X_{i,j} + X_{i - 1,j}}{\Delta z^2}$$

$$\frac{\partial X}{\partial z} \simeq \frac{X_{i + 1,j} - X_{i,j}}{\Delta z} \qquad [56]$$

Substituting Equation [53] and Equation [56] into Equation [40], we obtain

$$(D \cdot \Delta t - \bar{V} \cdot \Delta z \cdot \Delta t)X_{i + 1,j} - (2D \cdot \Delta t - \bar{V} \cdot \Delta z \cdot \Delta t + g(X_{i,j})\Delta z^2)X_{i,j} +$$

$$(D \cdot \Delta t)X_{i - 1,j} = - g(X_{i,j}) \cdot \Delta z^2 X_{i,j - 1} \qquad [57]$$

Equation [57] can be expressed as

$$AX_{i-1,j} + B_iX_{i,j} + CX_{i+1,j} = E_i \qquad [58]$$

where

$$A = D \cdot \Delta t$$

$$C = D \cdot \Delta t - \bar{V} \cdot \Delta z \cdot \Delta t$$

$$B_i = - (2D \cdot \Delta t - \bar{V} \cdot \Delta z \cdot \Delta t + g(X_{i,j}) \cdot \Delta z^2)$$

$$E_i = - g(X_{i,j}) \cdot \Delta z^2 \cdot X_{i,j-1}$$

Here, the value of $X_{i,j-1}$ is known. For each value of i, we can write one equation in the form of Equation [58]. For $i = 1$ to $i = N$, there are N equations and we need to compute N values of X. The N equations can be written in the matrix form as

$$
\begin{pmatrix}
B_1 & C & 0 & \cdot & \cdot \\
A & B_2 & C & 0 & \cdot \\
0 & A & B_3 & C & \cdot \\
\cdot & \cdot & \cdot & \cdot & \cdot \\
\cdot & \cdot & \cdot & \cdot & \cdot \\
\cdot & \cdot & \cdot & A & B_N
\end{pmatrix}
\cdot
\begin{pmatrix}
X_1 \\
X_2 \\
X_3 \\
\cdot \\
\cdot \\
X_N
\end{pmatrix}
=
\begin{pmatrix}
E_1 \\
E_2 \\
E_3 \\
\cdot \\
\cdot \\
E_N
\end{pmatrix}
\qquad [59]
$$

Equation [59] is solved by an implicit method described by Ames (1965) for $X_{i,j}$, ($i = 1,N$). In this equation, since $X_{i,j}$ is not known at the time of computation, $g(X_{i,j})$ cannot be evaluated before the computation. However, this can be determined by the predictor-corrector technique described below.

1. The $g(X_{i,j})$ is first approximated by $g(X_{i,j-1})$ and the solution of matrix [59] is made. This solution yields $X_{i,j}^1$ for $i = 1,N$. The superscript represents the number of iteration.

2. The $X_{i,j}^1$ now is used to evaluate $g(X_{i,j}^1)$ and the solution of matrix [59] is made again. This yields a better approximation of $X_{i,j}$ which is denoted as $X_{i,j}^2$.

3. This process of iteration is continued until the sum of $(X_{i,j}^n - X_{i,j}^{n-1})^2 \leq \varepsilon$ where ε is a tolerance limit. (ε was set at 10^{-5}).

4. The values $X_{i,j}^n$ are now the converged solution $X_{i,j}$ at time increment j. The computation of $X_{i,j+1}$ is done by repeating steps 1 through 4. A computation scheme for this method is shown in Figure 3b. This method is stable for a wide range of $\Delta t / \Delta z^2$, but the round-off error increases with decreasing Δz.

Some results will be compared between the two methods.

RESEARCH PLAN

The total study is divided into five experiments. The first two involve only theoretical and numerical study. The last three experiments involve both theoretical computation and experimental verification of the model.

Experiment 1
Study of the Numerical Methods

FORTRAN IV programs were written for the explicit method and for the implicit method and are described in the section of Materials and Methods. These programs are presented in Appendix A. The same set of parameters and exchange function were used to compute the concentration function $X(z,t)$ by the implicit method and by the explicit method. The purpose of this computation was to compare the results and the efficiency of the two methods.

Experiment 2
Study of the Effect of the Cation
Exchange Equilibria on the Cation Transport

Five selected exchange isotherms were used in the solution of material balance equation. The concentration functions $X(z,t)$ and $Y(z,t)$ that were obtained from each different exchange function were compared. This study was to examine the effect of the shape of the exchange isotherm on the pattern of ion transport.

Experiment 3
Comparative Study of the Linear Exchange
Model and the Non-linear Exchange Model

The Mg→Ca exchange reaction in Yolo fine sandy loam soil column was studied. The theoretical computation with a linear approach was compared to the one with a non-linear approach with respect to the exchange isotherm. This study was conducted to show that a proper description of the exchange function is essential for a good theoretical computation of the concentration function.

Experiment 4
Experimental Verification of the Model
for Mg→Ca Exchange in Soil Columns

The concentration functions $X(z,t)$ and $Y(z,t)$ were obtained experimentally and theoretically. These results were compared to prove that the model developed was applicable. The soils used were Hanford sandy loam and Nibley clay loam.

Experiment 5
Experimental Verification of the Model
for Na→Ca Exchange in Soil Columns

The Na→Ca exchange reaction in a Yolo fine sandy loam soil column was also studied. This study was conducted to observe the effect of isotherm shape on the exchange column performance. The Mg→Ca and the Na→Ca exchange differ greatly in their exchange function and consequently their concentration function $X(z,t)$ and $Y(z,t)$.

MATERIALS AND METHODS

The methods employed to evaluate cation exchange properties of the soils, the exchange isotherm, and the concentrations $X(z,t)$ and $Y(z,t)$ are described here. The parameters involved in Equation [40] which were evaluated are the soil properties Q, ρ, and α; the solution property C_o; and the flow parameters $\bar{V}$ and D. The exchange isotherm in the form of $Y = f(X)$ was also evaluated experimentally. To verify the applicability of the theoretical model, the laboratory experiment was conducted to determine the experimental values of $X(z,t)$ and $Y(z,t)$. The theoretical computation of $X(z,t)$ and $Y(z,t)$ from both the implicit and explicit methods were obtained from the results of the computer program.

Materials

Soils

Three different soils were used in the study, namely the Yolo fine sandy loam, Hanford sandy loam, and the Nibley clay loam. The Yolo soil was collected from the University of California farm at Davis, California. The Hanford soil was collected from the Kerney field station of the University of California near Fresno, California. The Nibley soil was collected from Utah State University's experimental farm, Providence, Utah. The soil properties for each column experiment will be presented in the results and discussion section of the dissertation.

Chemical solution

The chemical solution used in this study were 0.1 N $CaCl_2$, 0.1 N $MgCl_2$, and 0.1 N NaCl.

Column Setup

The physical structure of the column used in this study is shown in Figure 4. It consists of eleven lucite rings with an inner diameter of 7.6 cm and an outer diameter of 9.0 cm. The top ring is 4.5 cm in depth, whereas, the other ten rings are 2 cm in depth. The rings are put together by placing rubber gaskets between each ring. The bottom plate consists of a porous glass plate imbedded into a 1.3 cm thick lucite plate. There is an outlet at the center of this bottom plate. The whole column is bolted together by three threaded brass bars.

Laboratory Experiment

Column experiment

Soil was packed into the column uniformly to a depth of about 23 to 25 cm. The soil column was first saturated with Ca^{++} cation by establishing a steady flow of 0.1 N $CaCl_2$ solution. When saturation was attained, the column was used for the determination of the dispersion coefficient. This was done as following. The column was first flushed with a saturated $CaSO_4$ solution. Then the original $CaCl_2$ solution was reintroduced and the Cl^- breakthrough curve (BTC) obtained. The dispersion coefficient was calculated from the Cl^-
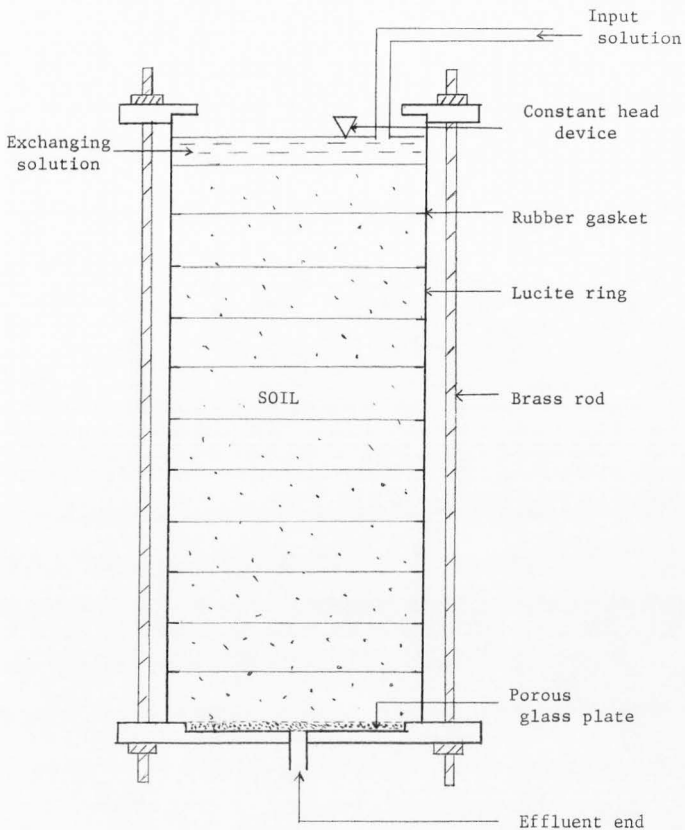
Figure 4. A sideview diagram showing the physical structure of the soil column used in this study.

BTC according to Equation [51]. Details will be shown in the next section. After the dispersion coefficient was determined and the column completely restored to the original concentration of 0.1 N $CaCl_2$, the cation exchange experiment was started by introducing an input (exchanging) solution of either 0.1 N $MgCl_2$ or 0.1 N NaCl without altering the steady state flow. After a predetermined quantity of the exchanging solution was introduced, the time was recorded and the flow was stopped. The column was immediately sectioned at the ring joints into eleven parts. The solution phase in each section was extracted under suction in a Buchner funnel. The soil was air-dried. The chemical composition of the solution extract and the exchangeable cations of the air-dried soil from each section was determined. The results obtained were $X(z,t)$ for the solution phase and $Y(z,t)$ for the exchanger phase.

Determination of the average interstitial flow velocity and the dispersion coefficient

The average interstitial flow velocity was obtained from the equation

$$\bar{V} = \frac{V}{A \cdot \alpha \cdot t} \qquad [60]$$

where V is the total volume of the solution passed through the column in the time period of t hours.

The dispersion coefficent was obtained by running a non-reactive anion through the steady state column and by obtaining the BTC. This process was described by Nielsen and Biggar (1961). A typical Cl^- BTC

is shown in Figure 5. The effluent volume at which the C/C_o of
Cl^- is 0.5 was designated as pore volume V_o. The slope of the BTC
at the one pore volume point was designated as S_o and the dispersion
coefficient was calculated from Equation [51].

Chemical analyses

The solution extract was diluted and the cation analyzed by an
atomic absorption spectrophotometer (Perkin Elmer, Model -303). For
the calcium and magnesium analyses, a Ca-Mg combination cathode tube
was used and the wavelengths were set at $4227\overset{o}{A}$ and $2852\overset{o}{A}$, respectively.
For the sodium analysis, a Na cathode tube was used at the wavelength
of $5870\overset{o}{A}$.

The process for analyzing exchangeable cations is described briefly
here. A 20-25 g soil sample was placed in a small leaching funnel and
washed with 350 ml of 95 percent alcohol until it was free of Cl^-. The
exchangeable cations were then extracted by leaching 450 ml of 1 N
CH_3COONH_4 through. The leachate was collected and diluted for analysis
of the cation on an atomic absorption spectrophotometer as was described
previously.

The chloride concentration was determined by the potentiometric
titration with 0.01 N $AgNO_3$ as the titrating solution. The Corning
Model 12 pH meter with an expanded scale was used. The electrodes used
are a glass electrode as a reference and the silver billet electrode as
the indicator electrode. The titration was carried out under a con-
stant acidic condition.

$$\frac{D}{V} = \frac{L}{4\pi V_o^2 S_o^2}$$

S_o : Slope

V_o
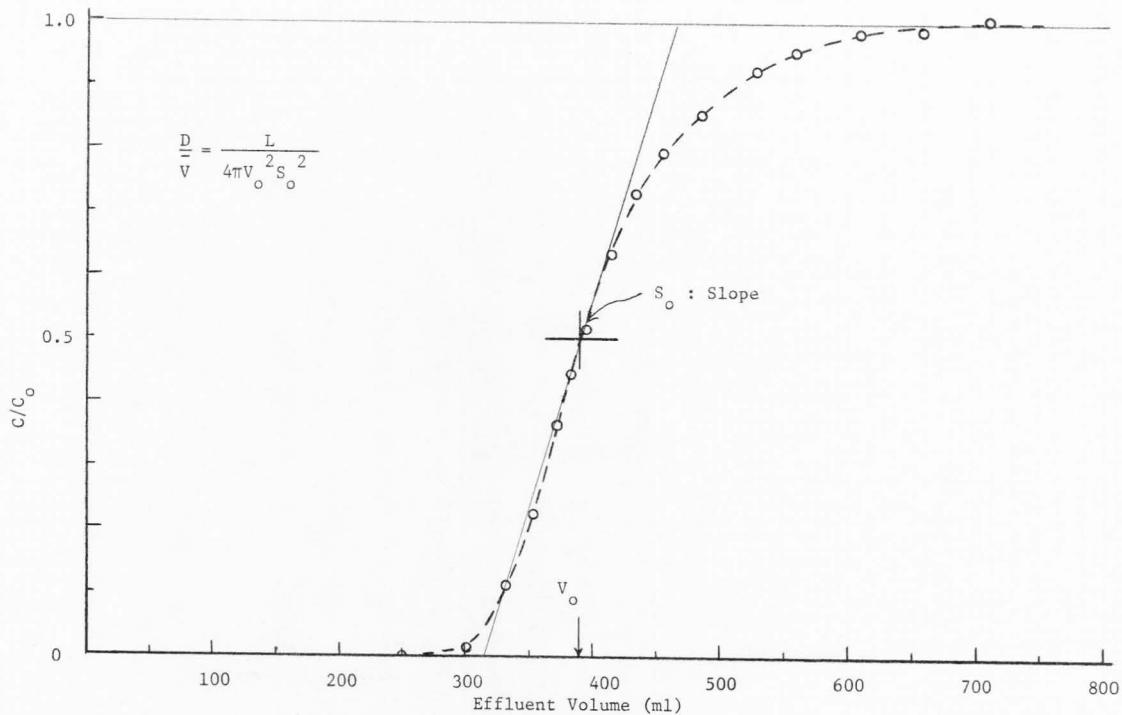
Figure 5. A typical Cl^- breakthrough curve used for calculating dispersion coefficient.

Exchange isotherm

The exchange isotherm was obtained by plotting the value of Y against its corresponding X value obtained from the same section of the column.

Cation concentration profiles

For the cation concentration profile of the solution phase, the X value was plotted against the mid-point depth of the corresponding section from which X was determined. For the cation concentration profile of the exchanger phase the Y value was plotted against the midpoint depth of the corresponding section from which the Y was determined.

Computer Experiment

The digital computer used for this study was a Univac Model 1108, located at the Computer Center of the University of Utah, Salt Lake City. The FORTRAN programs were run via a remote terminal at the Engineering building, Utah State University. The remote terminal consists of a card reader and a printer which handles the Input/Output of the computing process.

Two major programs were written for this study. They are the program for the explicit method and the program for the implicit method. These methods were described in the theoretical development section. The outlines of each program are described in the following sections.

The program for the explicit method

1. Input: Read in the parameters D, $\bar{V}$, ρ, Q, α, and C_o for each column experiment.

2. Set the initial condition $X_{i,0} = 0$ for (i = 1,n) where i is the depth increment.

3. Set the boundary condition $X_{0,j} = 1.0$ for j = 1,m, where m is the last time increment.

4. Begin the computation of $X_{i,1}$ for the time period 1 using the computation scheme presented in Equation [54].

5. Evaluate the bottom boundary value $X_{n+1,1} = X_{n-1,1}$.

6. Output: Print out the values $X_{i,1}$.

7. Repeat steps 4 to 6 to compute X of the subsequent time increment.

8. End the computation.

The flow diagram of this program is shown in Figure 6. The actual program is presented in Appendix A.

The program for the implicit method

1. Input: Read in the parameters D, $\bar{V}$, ρ, Q, α, and C_o for each column experiment.

2. Set the initial condition $X_{i,0} = 0$ for i = 1,n.

3. Set the boundary condition $X_{0,j} = 1.0$ for j = 1,m, where m is the last time increment.

4. Start the computation of $X_{i,j}$ at this time period.

    a) Evaluate the coefficient matrix of Equation [58].

    b) Follow the predictor-corrector method described on page 31 to solve the matrix of Equation [59].
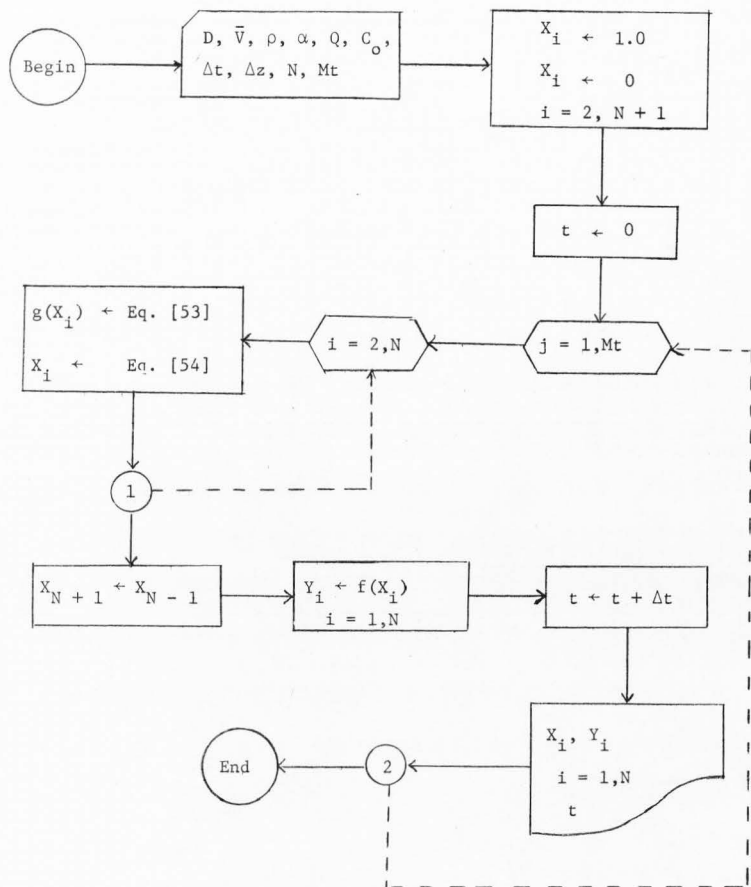
Figure 6. The flow diagram for the explicit method of computation.

5. Output: Print out the converged value of $X_{i,j}$.

6. To compute X for the next time increment, repeat the procedure from step 4 to step 6.

7. End the computation.

The flow diagram of this computer program is presented in Figure 7. The actual program used is presented in Appendix A.

Begin

D, $\bar{V}$, ρ, α, Q, C_o, Δt, Δz, ε, N, Mt

$X_i \leftarrow 1.0$
$X_i \leftarrow 0$
$i = 2, N + 1$

$t \leftarrow 0$

$j = 1, Mt$

$B_i \leftarrow$ Eq. [58]
$E_i \leftarrow$ Eq. [58]

$i = 1, N + 1$

1

2

3

$X_i \leftarrow$ TDMX
details on page 45

4

$X_i^{n+1} - X_i^n < \varepsilon$

F

T

$Y_i \leftarrow f(X_i)$

$t \leftarrow t + \Delta t$

X_i, Y_i
$i = 1, N$
t

End
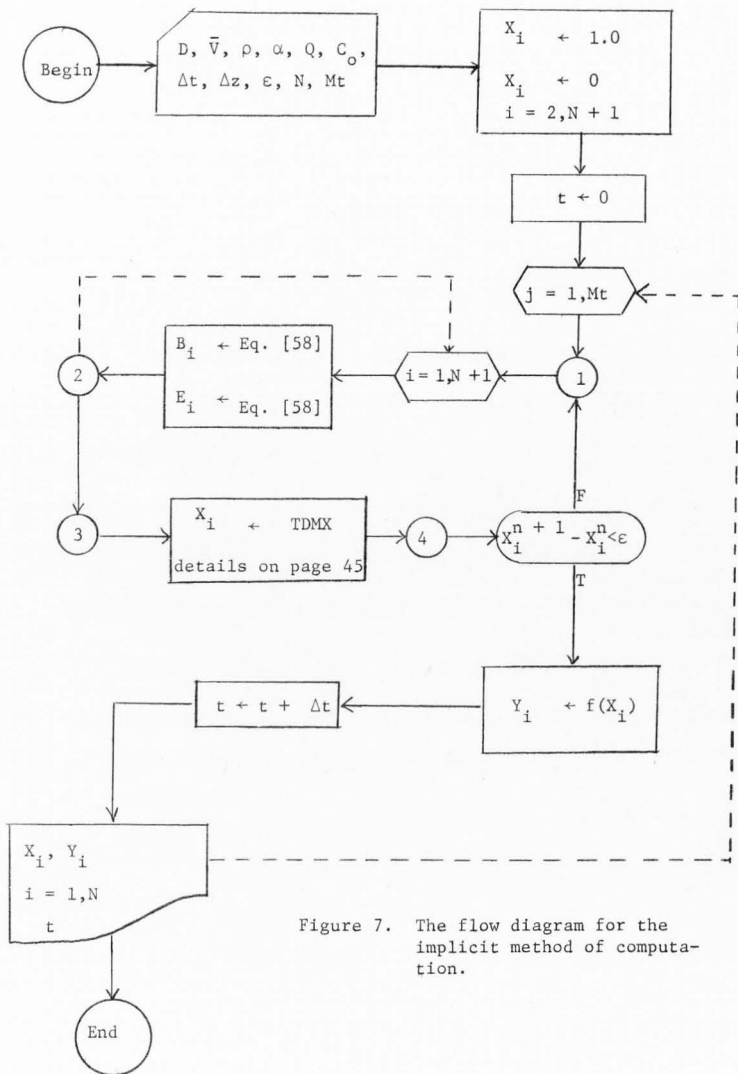
Figure 7. The flow diagram for the implicit method of computation.
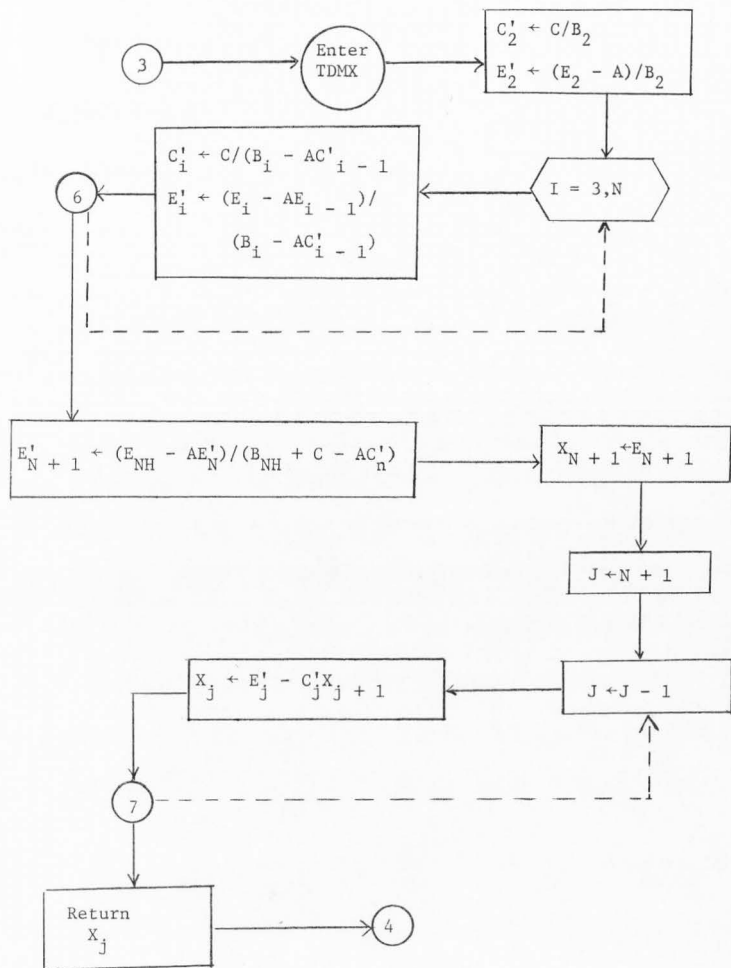
Figure 7. Continued, showing the details of the subroutine TDMX.

RESULTS AND DISCUSSION

Experiment 1
Study of Numerical Methods

The purpose of this experiment was to compare the mathematical solution of the same cation transport problem obtained from two different methods, the explicit method and the implicit method.

The isotherm selected for this experiment is shown in Figure 8d. The exchange function has the form

$$Y = \frac{X}{X + (1 - X)\ \text{Exp}[c(1 - 2X)]} \qquad [61]$$

where $c = -1$. The selected properties of the soil exchanger, the solution, and the flow parameters are listed in Table 1.

Table 1. The basic column and soil parameters used in Experiment 1 and Experiment 2

Flow velocity cm/hr.	1.50
Dispersion coefficient cm^2/hr.	1.50
Bulk density g/cm^3	1.30
Pore fraction	0.45
Cation exchange capacity me/g	0.25
Column length cm	30.00
Pore volume ml	612.5
Total Cation concentration me/ml	0.10
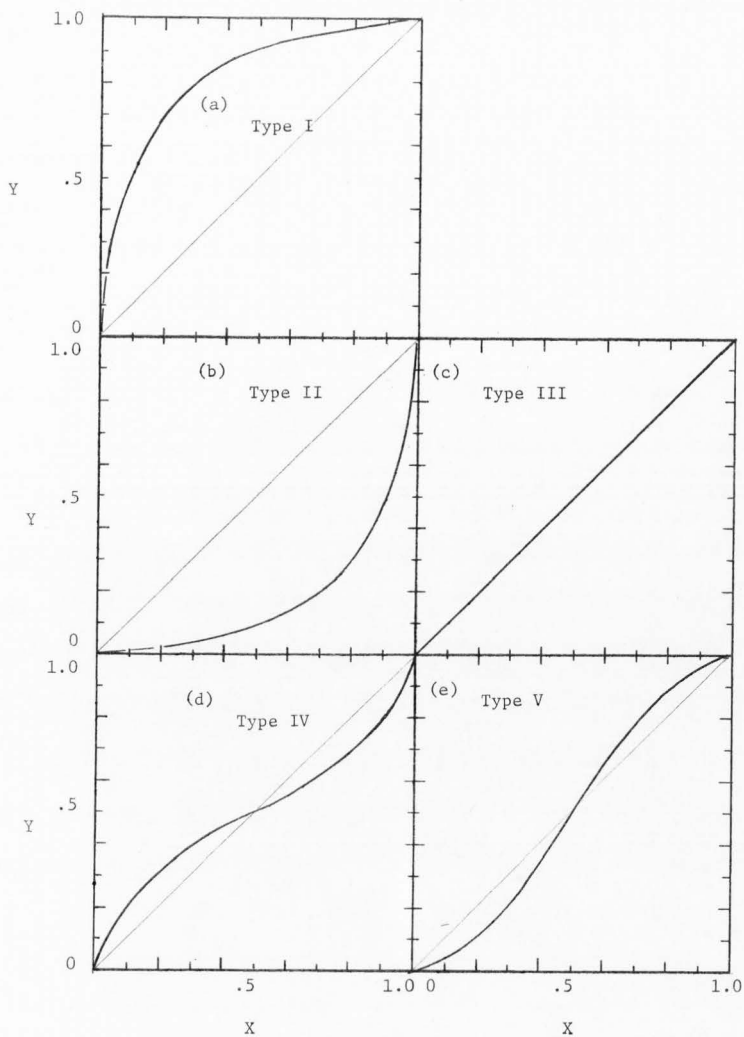
Figure 8. Five different types of the idealized isotherm used in Experiment 1 and Experiment 2.

The explicit method

In using the explicit method, it is necessary that $0 < \Delta t/\Delta z^2 \leq 1/2$. This condition restricts the choice of the values for Δt and Δz. In this study, Δt was set at 0.1 hour and Δz at 0.5 cm. The solution of $X(z,t)$ is presented in Figure 9 as a X vs z plot with time as a parameter.

The implicit method

The applicability of this method was not restricted by the value of $\Delta t/\Delta z^2$. The convenient values of $\Delta t = 0.5$ hour and $\Delta z = 0.2$ cm were used. The solution $X(z,t)$ is presented in Figure 9 along with the results obtained from the explicit method.

It is clear from Figure 9 that the solution obtained from these two methods are almost identical despite the different values of Δt and Δz used. Thus, accuracy is not a factor in considering the superiority of the two methods. However, the practical factors of computer time and the storage requirement used in the computation are quite different for the two methods.

For the explicit method, the computer execution time for solving this problem was approximately 6 seconds. On the other hand, the implicit method took approximately 24 seconds. The storage requirement for the explicit method was approximately 3 to 5 times less than that of the implicit method. These differences are due to the fact that the implicit method involved solving a tridiagonal matrix with two vectors consisting of variable coefficients which needed to be stored before the system could be solved. Futhermore, the implicit
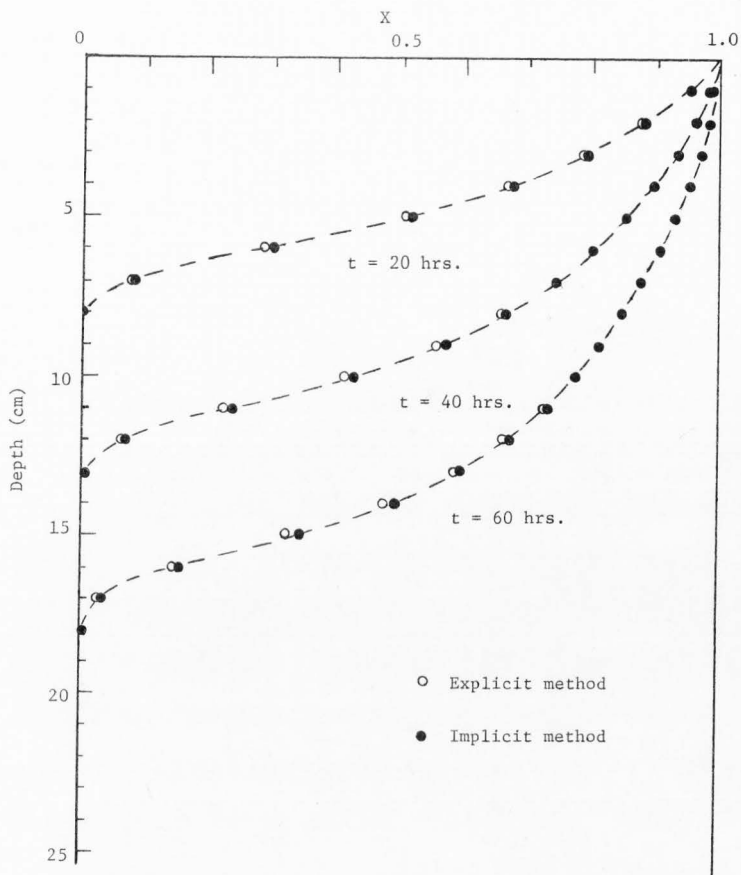
Figure 9. Concentration profiles computed from the explicit method and implicit method.

method requires two arrays of working area to store the solution during the iteration process in order to provide a test of convergence.

Considering the two factors of computer time and storage requirement, it was less expensive to use the explicit method while still preserving the accuracy of the solution. Thus, the explicit method was used throughout the study.

<div style="text-align:center">

Experiment 2
Study of the Effect of the Cation Exchange
Equilibria on the Cation Transport

</div>

Exchange function and exchange isotherm

Five selected cation exchange isotherms were studied. These isotherms are designated as Type I, II, III, IV, and V as shown in Figure 8 a, b, c, d, e, respectively. The first three types belong to the "regular" system. Their exchange functions are expressed by Equation [44] with S_B^A equal to 10, 0.1, and 1, respectively. Types IV and V belong to the "irregular" system. Their exchange functions are represented by Equation [48] with the value of ln K equal to 0 for both types and the value of c equal to -1.0 and 1.2, respectively.

Concentration functions $X(z,t)$ and $Y(z,t)$

In Equations [53] and [54] the solution of the concentration function $X(z,t)$ involved the term $g(X)$ which contains $f'(X)$. The term $f'(X)$ denotes the slope of the exchange isotherm. For each type of the isotherms shown, a set of solutions for $X(z,t)$ and $Y(z,t)$ was obtained. Discussion of the functions $X(z,t)$ and $Y(z,t)$ obtained

from the five different types of isotherms are presented separately in the following sections.

Type I. The characteristic of the Type I isotherm is that it possesses a large separation factor ($K' = 0.1$ or $S_B^A = 10$). Within the entire concentration range of 0 to 1 that was studied, the tendency for the cation to be adsorbed was stronger than the tendency of it to remain in the solution. This effect is also manifested in the functions $X(z,t)$ and $Y(z,t)$. Careful examination of Figure 10 (a,b) reveals that the advancement of the concentration function $Y(z,t)$ is always ahead of the function $X(z,t)$ within the entire concentration range. At a particular depth of the column, when the concentration of the solution X reaches 0.5, the concentration of the exchanger Y is approximately 0.92. Another characteristic of the concentration functions $X(z,t)$ and $Y(z,t)$ is that they possess a sharp boundary.

These two characteristics tend to make the "cation filtration" effect very efficient. This point will be more apparent when the results of the other types of cation exchange are examined later. A practical example of this type of reaction occurring in a soil system is the Ca→Na exchange. The softening of hard water by ion exchange is another practical example of Type I.

Type II. The character of the isotherm of this type (which is shown in Figure 8b) is that it possesses a weak separation factor ($K' = 10$ or $S_B^A = 0.1$). Thus, the tendency of the cation to remain in the solution phase is stronger than the tendency of the cation to be adsorbed. This effect is also carried onto the concentration
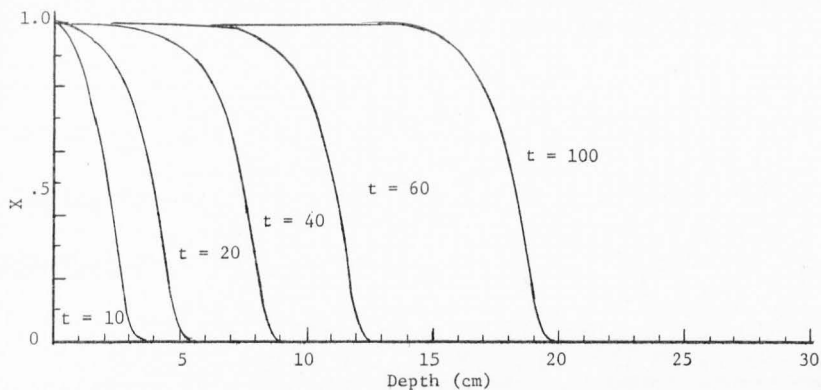
Figure 10a. Concentration profiles X(z,t) computed from the Type I isotherm.
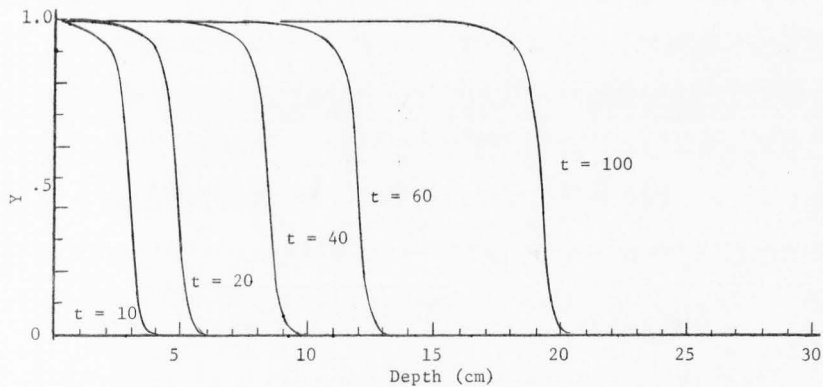
Figure 10b. Concentration profiles Y(z,t) computed from the Type I isotherm.

functions $X(z,t)$ and $Y(z,t)$. Examination of Figures 11a and 11b reveal
that the concentration profile of $X(z,t)$ stays ahead of that of $Y(z,t)$
at all times and in the entire concentration range. It is also noticed
that the boundaries of the concentration profiles are very diffused.
All these behavior patterns are much different from those resulted from
the Type I isotherm.

A Type II exchange reaction is considered to be "leaky." It is
very inefficient in the cation saturation operation. In other words,
it will take a great deal of cation solution to pass through the
column in order to obtain saturation with the exchanging cation. A
practial example for this type of reaction is that of the exchange
$Na \rightarrow Ca$. Because of the low selectivity coefficient of Na^+ against
Ca^{++} or Mg^{++}, much of the Na^+ was carried out of the soil system
before it could be adsorbed on the soil exchanger. From the agricul-
tural standpoint, this is a rather fortunate fact since accumulation
of Na^+ in the soil system makes the soil properties deteriorate and
is not desirable for the growth of a normal plant.

Type III. The characteristic of this type of exchange isotherm
which is shown in Figure 8c is that it has a unit separation factor
($S_B^A = 1$). Therefore, the tendency of the cation to be adsorbed is
identical to the tendency for it to remain in the solution. This
unique situation is reflected in the result of the concentration
functions $X(z,t)$ and $Y(z,t)$. It is noticed that the concentration
profiles presented in Figure 12 are for both $X(z,t)$ and $Y(z,t)$ be-
cause at any time and depth, they are identical. These profiles
take a smooth S-shaped curve.
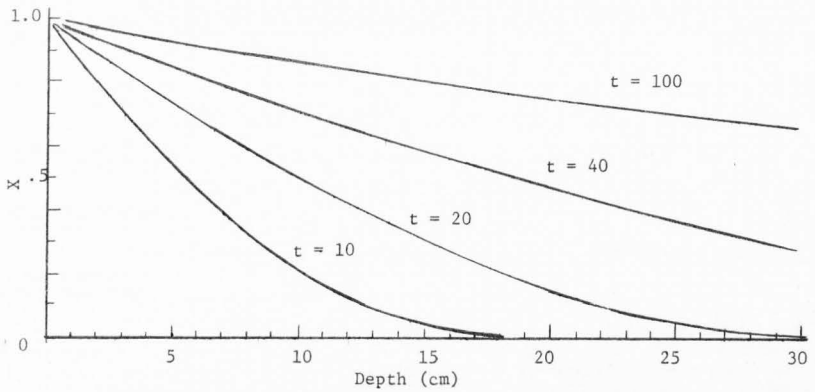
Figure 11a. Concentration profiles $X(z,t)$ computed from the Type II isotherm.
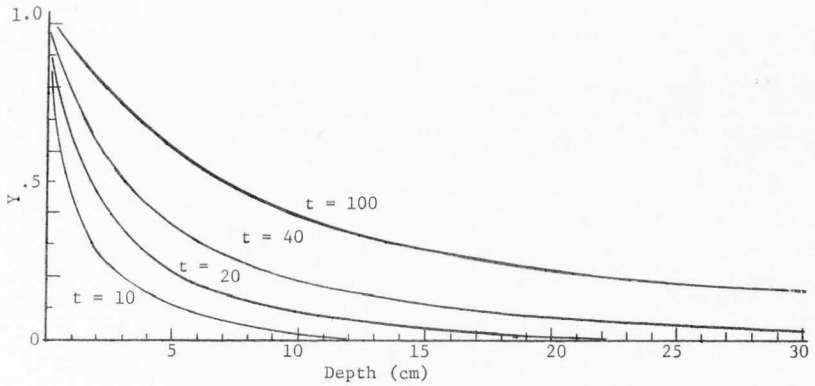
Figure 11b. Concentration profiles $Y(z,t)$ computed from the Type II isotherm.
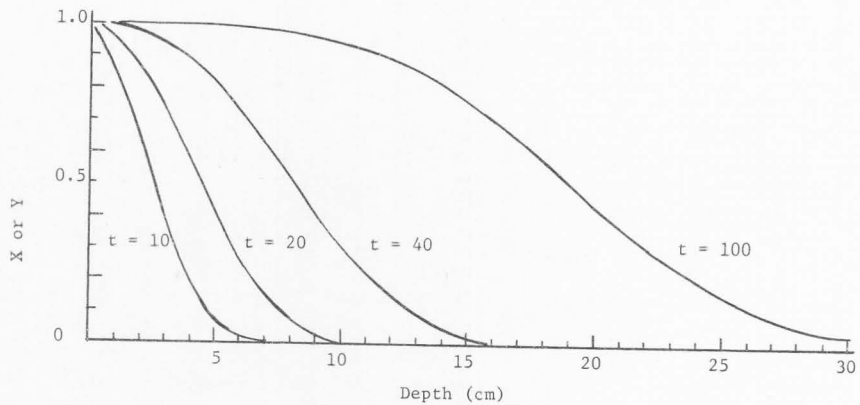
Figure 12. Concentration profiles $X(z,t)$ and $Y(z,t)$ computed from the Type III isotherm.

In reality, this type of isotherm is rather rare. One example of this type is the isotopic exchange. The reason for treating this type of reaction here is mainly to make it a reference in comparing other types of cation exchange reactions.

Type IV. The character of this type of isotherm which is shown in Figure 8d is that it possesses a non-constant separation factor and rather, the separation factor is a function of the solution concentration. Qualitatively, the value of the separation factor is greater than 1 in the region $0<X<0.5$, and is less than 1 in the region $0.5<X<1.0$. The effect of the characteristics of the isotherm on the result of concentration functions is noted in Figures 13a and 13b.

The concentration profile can be divided into two parts according to their shapes. In the region $X<0.5$, the shape of the profiles resemble that of Type I. In the region $X>0.5$, the shape of the profiles resemble that of Type II. It is also noticed that in the region of $X<0.5$, $Y(z,t)$ advances ahead of $X(z,t)$. On the contrary, in the in the region $X>0.5$, $Y(z,t)$ lags behind of $X(z,t)$. These consequences are the results of the change in the value of the separation factor with the concentration.

The exchange reaction of $Mg+Ca$ in some soils belongs to this type. Examples will be studied in Experiment III and IV. A more detailed discussion of these examples will be delayed until the corresponding experiments are treated.

Type V. The characteristics of the isotherm of Type V are qualitatively reverse of that of Type IV. The separation factor
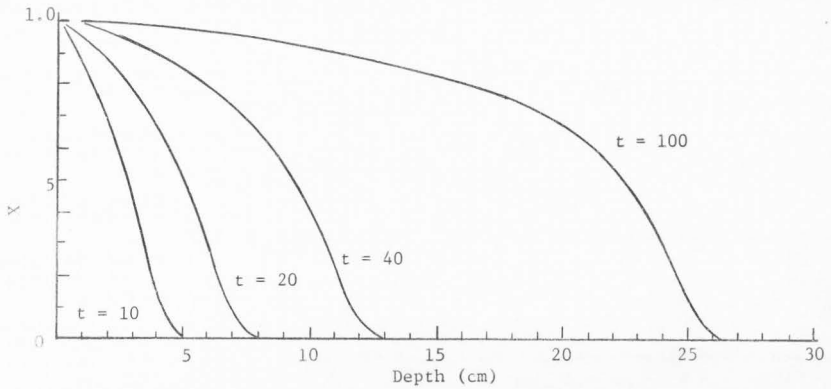
Figure 13a. Concentration profiles X(z,t) computed from the Type IV isotherm.
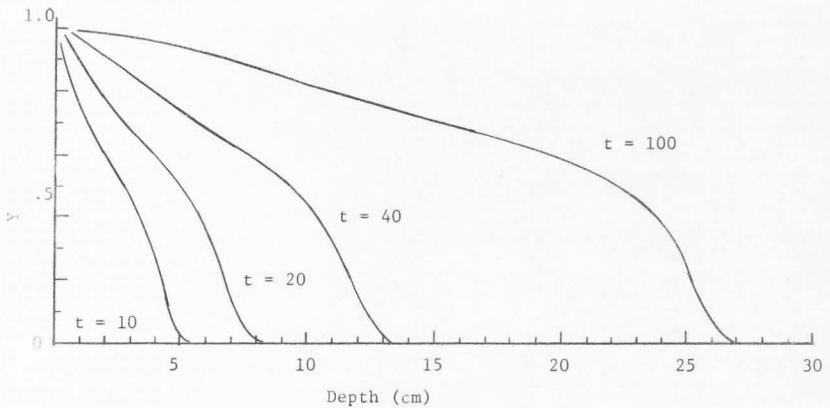
Figure 13b. Concentration profiles Y(z,t) computed from the Type IV isotherm.

varies with concentration. In the region of $X<0.5$, the separation factor is less than one. Whereas, in the region of $X>0.5$, the separation factor is greater than one.

It is shown in Figures 14a and 14b that the concentration profiles behave like Type I in the region of $X>0.5$ and behave like Type II in the region $X<0.5$. This behavior is a reverse of that of Type IV. That is, the concentration boundary is sharp when $X>0.5$ and is diffused when $X<0.5$. Another consequence of the varying separation factor is that the concentration profile $X(z,t)$ advances ahead of $Y(z,t)$ when $X<0.5$ and the opposite is true for $X>0.5$.

An example of this type was found by Peterson et al. (1965) in the exchange of $Mg \to Ca$ in a vermiculite.

Summary of Experiment II

What has been shown in this experiment can be summarized as follows:

1. The shape of the concentration functions $X(z,t)$ and $Y(z,t)$ is influenced by the separation factor in such a way that for $S_B^A>1$, these functions $X(z,t)$ and $Y(z,t)$ show a sharp boundary compared to those for $S_B^A = 1$ (Type III). On the contrary, for $S_B^A<1$, the opposite is true.

2. The relative advancement of the profile $X(z,t)$ and $Y(z,t)$ is governed by S_B^A in such a way that for $S_B^A>1$, $X(z,t)$ will lag behind $Y(z,t)$ and for $S_B^A<1$, $X(z,t)$ will advance ahead of $Y(z,t)$.

3. With $S_B^A = 1$, the value of $X(z,t)$ and $Y(z,t)$ are identical, and they exhibit a smooth S-shaped curve.
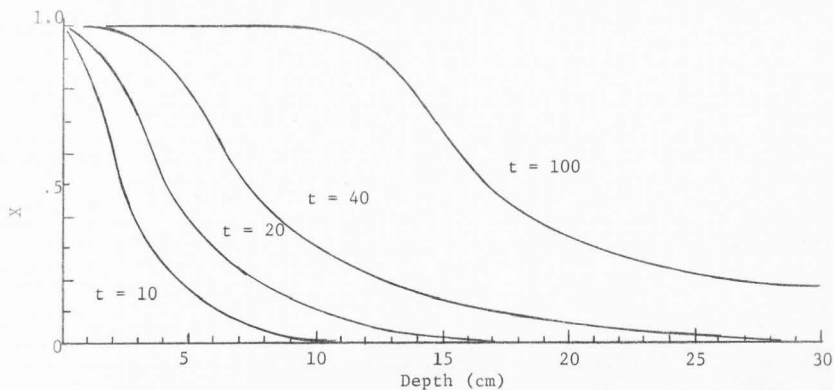
Figure 14a.   Concentration profiles X(z,t) computed from the Type V isotherm.
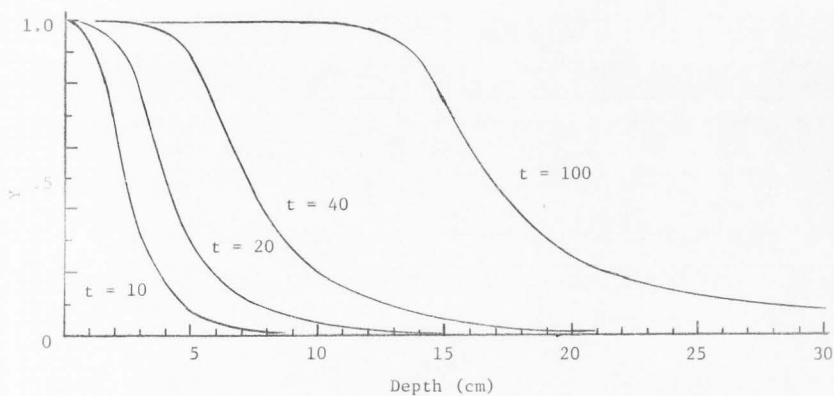
Figure 14b.   Concentration profiles Y(z,t) computed from the Type V isotherm.

Experiment 3
Comparative Study of the Linear Exchange
Model and the Non-linear Exchange Model

This experiment was intended to compare the linear approach of the Lapidus and Amundson model with the non-linear approach pursued in this study. Column experiments were conducted for the cation exchange of Yolo fine sandy loam soil. The three sets of experimental column data were then compared with the theoretical computation from the linear approach and from the non-linear approach.

The parameters involved in the three column experiments are listed in Table 2. The three column treatments differed mainly in the total input (exchanging) volume and hence the depth of miscible displacement. These data were used for the input data in the theoretical computation. The cation exchange isotherm for the Mg→Ca is presented in Figure 15. In each section of the columns, a value of X was associated with a corresponding value Y and the isotherm was constructed by plotting Y against X. The X and Y values from the experiment were fitted into a linear regression equation for the theoretical computation of the linear method. The linear regression equation is as follows:

$$Y = 0.04 + 0.92X$$

The same values were used to obtain the constants involved in Equation [48] as follows:

$$Y = \frac{X}{X + (1 - X) \, \text{Exp} \, [\ln K + c(1 - 2X)]} \qquad [48]$$

Table 2. The basic column and soil parameters for Experiment 3

Items		Column		
		3-I	3-II	3-III
Soil: Yolo fine sandy loam				
Flow velocity	cm/hr	3.936	4.712	3.688
Dispersion coefficient	cm^2/hr	1.875	2.245	1.757
Bulk density	g/cm^3	1.284	1.295	1.303
Pore fraction		0.406	0.406	0.441
Cation exchange capacity	me/g	0.257	0.262	0.274
Total concentration	me/ml	0.105	0.104	0.105
Column length	cm	24.7	24.7	23.6
Total time	hr	14.	25.	40.
Pore volume	ml	455.	455.	472.
Total input volume	ml	1015.	2170.	2950.
Total input volume	(pore volume)	2.2311	4.7700	6.2481

where the value of ln K and c were found to be 0.0855 and -0.475, respectively. The later Kielland exchange function (Equation [48]), which was referred to by Helfferich (1962), was used in the theoretical computation of the non-linear method.

The cation concentration profiles $X(z,t)$ and $Y(z,t)$ from the column experiments are presented in Figures 16a and 16b, respectively. The same graphs also contain the concentration profiles computed from the linear and non-linear methods.
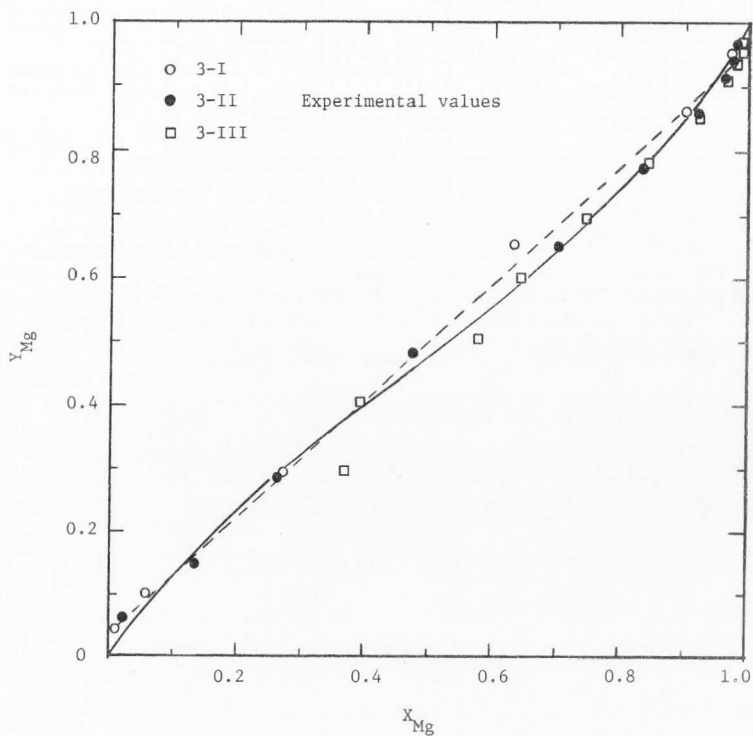
Figure 15. The cation exchange isotherm for the exchange of Mg→Ca in
Yolo fine sandy loam soil. Experimental values are repre-
sented by spots. The broken line is the linear regression
line. The solid line shows the Kielland exchange function.
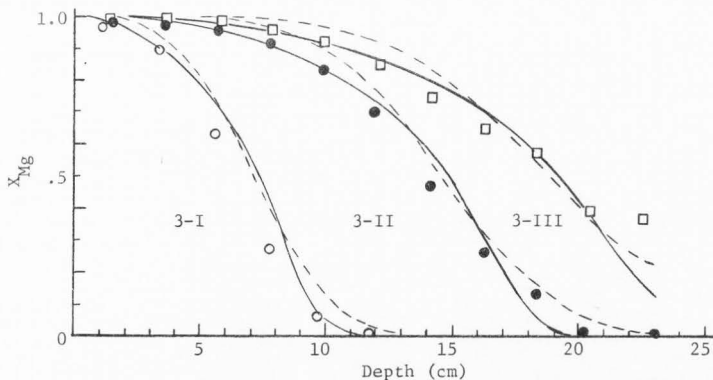
Figure 16a.   Concentration profiles $X(z,t)$ for Mg^{++} include experimental values shown by the spots and theoretical computation. The broken lines show the values computed from the linear method. The solid lines show the values computed from the non-linear method.
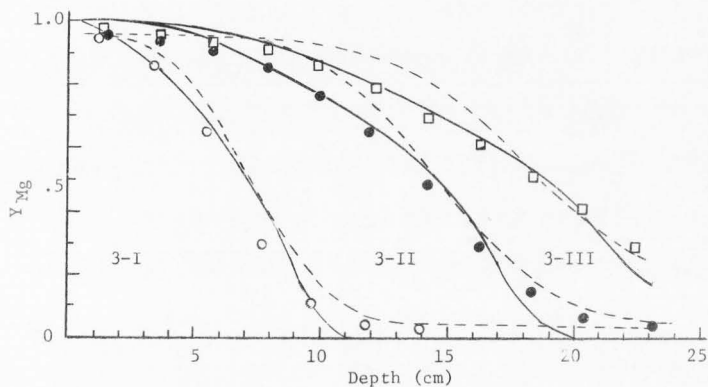
Figure 16b.   Concentration profiles $Y(z,t)$ for Mg^{++} include experimental values shown by the spots and theoretical computation. The broken lines are computed from the linear method. The solid lines are computed from the non-linear method.

From Figures 16a and 16b, it is noted that the concentration pro-
files computed from the non-linear model (represented by the solid
lines) agree with the experimental profiles better than the ones from
the linear model (represented by the broken line) both in the shape of
the profiles and in the actual position of the profiles. This trend
is most apparently shown on the higher concentration part of the pro-
files.

A reference of the exchange isotherm in Figure 15 shows that the
non-linear fit of the isotherm represents the actual experimental
values more closely than the one from the linear model. This is more
so in the concentration range of 0.4 to 1.0.

At first glance, it was rather surprising to see the improvement
of the theoretical computation of $X(z,t)$ and $Y(z,t)$ resulting from such
a slight adjustment of the isotherm from the linear one to the non-
linear one considering the very slight difference in the actual posi-
tion of the two isotherms. A more careful examination of the theroetical
development revealed that the theoretical calculation involved the
slope of the isotherm rather than the actual position of the isotherm.
Thus the difference in the shape of the concentration profiles $X(z,t)$
and $Y(z,t)$ is justified considering the apparent differences of the
slope of the isotherm between the linear one and the non-linear one,
especially at the higher concentration portion of the profiles.

It was mentioned in the literature review that the study by
Bigger and Nielsen (1963) pointed out that one of the reasons for the
disagreement of the Lapidus and Amundson model from the experimental

data could be due to an inadequate description of the exchange function. This experiment gives evidence to support their reasoning that an improvement of the exchange function improves the theoretical model.

<div align="center">

Experiment 4
Experimental Verification of the Model
for Mg→Ca Exchange in Soil Columns

</div>

This experiment deals with the Mg→Ca exchange in soil columns undergoing miscible displacement in a steady flow condition. Two different soils were used to study and test the applicability of the theoretical model developed in this study. Three column experiments were conducted with each soil, each with an increasing amount of exchanging solution input.

From the column experiments, three types of data were obtained, namely:

1. The basic parameters describing soil properties, solution compositions, and flow characteristics.

2. The cation exchange isotherms.

3. The cation concentration profiles for the solution phase and the exchanger phase.

The results will be presented and discussed separately with respect to the two different soils.

Nibley clay loam

The experimentally determined values of the basic parameters from the three column experiments are listed in Table 3. The cation exchange isotherm in terms of the equivalent fraction is shown in Figure 17. The

Table 3. The basic column and soil parameters for Experiment 4

Items	Unit	Columns		
		4-I	4-II	4-III
Flow velocity	cm/hr	1.0428	1.2269	1.9739
Dispersion coefficient	cm^2/hr	1.2680	1.4919	1.4706
Bulk density	g/cm^3	1.3320	1.3320	1.3073
Pore fraction		0.4456	0.4456	0.4670
Cation exchange capacity	me/g	0.2662	0.2845	0.3080
Total concentration	me/ml	0.1069	0.1106	0.1111
Column length	cm	23.5	23.5	23.6
Total time	hr	20.	50.	50.
Pore volume	ml	475.	475.	500.
Total input volume	ml	430.	1240.	2090.
Total input volume	(pore volume)	0.9053	2.6108	4.1800

Soil: Nibley clay loam

experimental values were fitted into a curve in the form of Equation [48] where the value of ln K and c were 0.4048 and -0.92, respectively for Nibley clay loam. The concentration profiles data from the column experiments and from the theoretical computation are presented in Figures 18a and 18b for $X(z,t)$ and $Y(z,t)$, respectively.

It is clearly seen from Figure 17, that the exchange isotherm is non-linear. However, one could argue that a linear regression line could be fitted just as well as a non-linear one. However, the linear regression line will not pass the two diagonal points with X and Y
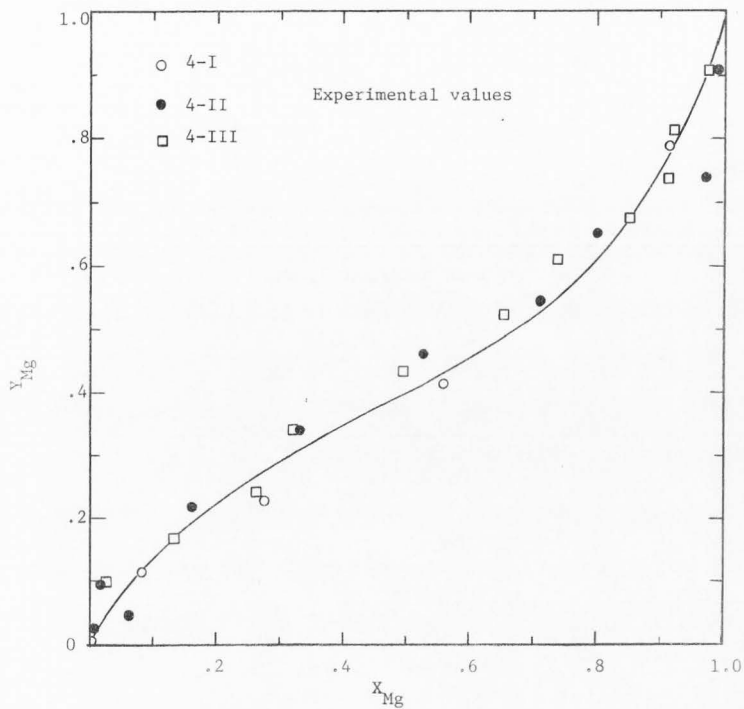
Figure 17. The Kielland cation exchange isotherm for the exchange of Mg→Ca in Nibley clay loam soil shown by the solid line, along with experimental data from three column experiments represented by the spots.
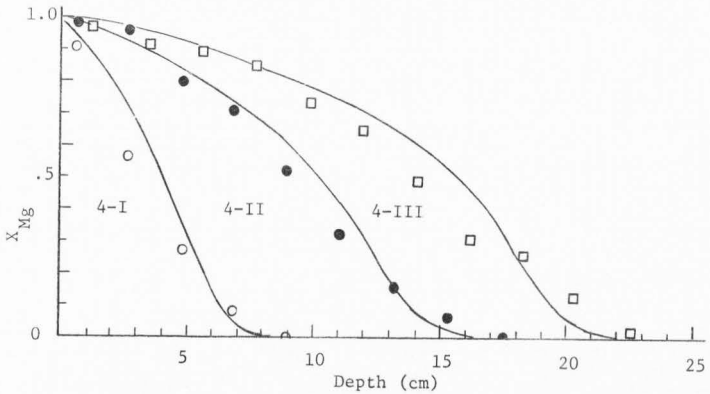
Figure 18a. The concentration profiles X(z,t) from three column experiments for Nibley clay loam soil, as shown by the spots, with theoretically computed values shown by the solid line.
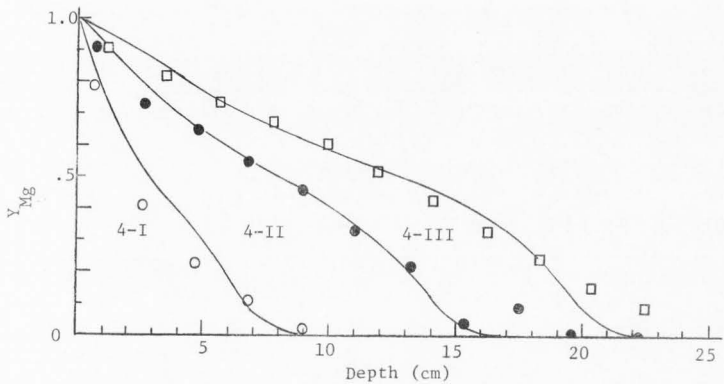
Figure 18b. The concentration profiles Y(z,t) from three column experiments for Nibley clay loam soil, as shown by the spots, with theoretically computed values shown by the solid line.

having coordinates of (0,0) and (1,1). In this particular case, this is not allowed by the theory of cation exchange. Therefore, a linear approach is not adequate. This point was demonstrated in Experiment 2.

Examination of Figures 18a and 18b reveals that the theoretical model actually does predict the column experiment data in both the shape of the profiles and in the extent of the cation penetration. It should be noted, however, that the slightly over-predicted profile could probably be attributed to the slight deviation of the theoretical exchange function from the actual one. In Figure 17, the theoretical exchange function lies below the actual data in the range of $0.3 < X < 0.9$. Therefore, the theoretical model actually allows more of the exchanging cation (Mg) to move down the column without exchanging with Ca.

In the deeper part of the profiles, it is also noted that the theoretical values lag behind that of the actual ones. This descrepancy could be caused by several possible factors. First, the equilibrium condition may not be approached completely and uniformly before the solution passes onto the deeper depth. This effect which is sometimes called "channeling" effect could cause more spreading in the concentration profiles. Second, the value of the dispersion coefficient which was determined experimentally with the non-reactive anion may not be the same as that was operative during the cation displacement experiment. An underestimated dispersion coefficient could make the theoretically computed profiles sharper than that of the experimental ones. Other possible sources of error such as the one in the chemical analysis and the one caused in the numerical computation cannot be ruled out.

Hanford sandy loam

The data listed in Table 4 are parameters determined from the three column experiments for the Hanford sandy loam. The experimental values of the exchange isotherm and the theoretically fitted exchange function are presented in Figure 19. The values of ln K and c for this exchange are 0.377 and −0.725, respectively. The cation concentration profiles for the solution phase and for the exchanger phase are presented in Figure 20a and Figure 20b, respectively.

The non-linear behavior of the exchange function is once again clearly shown in Figure 19. The data points from the three column experiments plotted in this figure follow a similar pattern. However, it is felt that too few data points were obtained at the lower concentration range of the isotherm.

The concentration profiles shown in Figure 20a and Figure 20b appear to be in general agreement between the theoretically calculated values and those experimentally determined. The slight discrepancy could be due to the deviation of the exchange function from the actual one at the lower concentration range since not enough data points were obtained. Other possible causes of the discrepancy were discussed in the previous section.

In this experiment, several things were noted. First, the cation exchange isotherms for the exchange reaction $Mg \rightarrow Ca$ at the total concentration of 0.1 N were not linear for the soils studied. The isotherms of this experiment qualitatively resembled those of Type IV of Experiment 2. Second, the model proposed in this study, in general, predicts the cation transport in soil column with reasonable accuracy. The

Table 4.   The basic column and soil parameters for Experiment 4.

| Items | Unit | Column | | |
		4-I	4-II	4-III
		Soil: Hanford sandy loam		
Flow velocity	cm/hr	1.2840	1.3024	1.4521
Dispersion coefficient	cm^2/hr	0.3160	0.3272	0.4807
Bulk density	g/cm^3	1.6019	1.6043	1.5905
Pore fraction		0.3582	0.3509	0.3784
Cation exchange capacity	me/g	0.0568	0.0586	0.0629
Total concentration	me/ml	0.1077	0.1084	0.1068
Column length	cm	24.0	24.5	22.6
Total time	hr	15.	30.	43.
Pore volume	ml	390.	390.	388.
Total input volume	ml	313.	622.	1072.
Total input volume	(pore volume)	0.8025	1.5948	2.7632

concentration profiles are similar to that of Type IV of Experiment 2.
Third, the equilibrium assumption may not strictly hold due to the
possible "channeling" effect of the exchanging cation solution. For an
overall prediction of the cation transport, the equilibrium assumption
is, however, practical provided that the interstitial flow velocity of
the cation solution is not extremely fast compared to the rate of cation
exchange and that it is allowed to approach the equilibrium between the
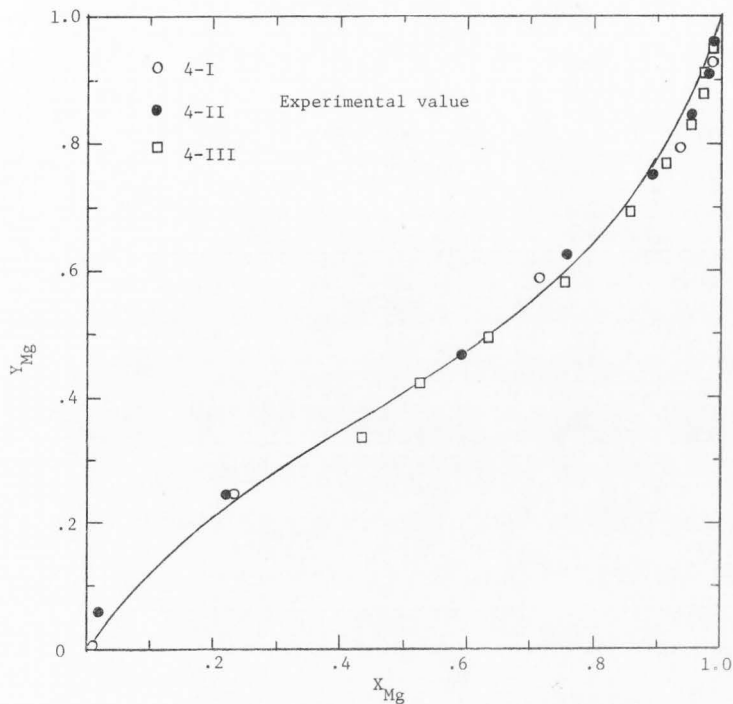
Figure 19. The Kielland cation exchange isotherm for the exchange Mg→Ca in Hanford sandy loam soil, along with the experimental data from three column experiments.
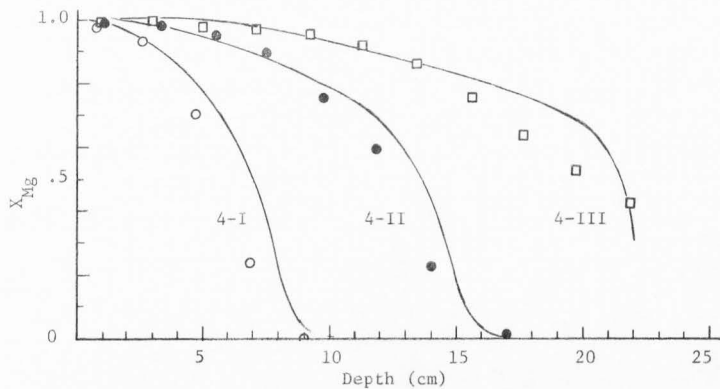
Figure 20a. The concentration profiles $X(z,t)$ from three column experiments for Hanford sandy loam, with the theoretically computed values shown by the solid lines.
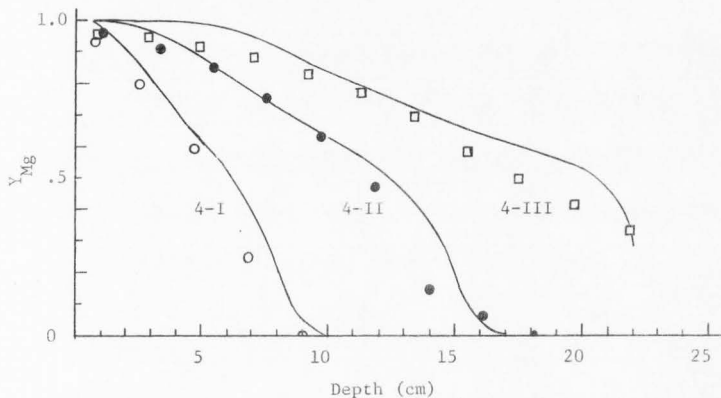
Figure 20b. The concentration profiles $Y(z,t)$ from three column experiments for Hanford sandy loam, with the theoretically computed values shown by the solid lines.

solution phase and the exchanger phase. This situation usually pre-
vails in cation movement through a soil body.

Experiment 5
Verification of the Model for the
Na→Ca Exchange in Soil Columns

This experiment was set up to verify the model of cation trans-
port for the Type II exchange isotherm discussed in Experiment 2.
The experimental parameters are listed in Table 5. The Yolo fine sandy
loam soil was used in this experiment.

The experimentally determined isotherm for this experiment obtained
from three soil column runs are presented in Figure 21. This isotherm
appears to be very similar to the example treated in Experiment 2, Type
II. Therefore, a "regular" exchange function was fitted as shown by the
dotted line in Figure 21. This exchange function is written in the
following equation

$$Y = \frac{X}{X + (1 - X) \ K'} \qquad [44]$$

where $K' = 9$. A careful examination of this function shows that the
theoretical function overestimates Y in the concentration range of
$0.7 < X < 1.0$ while it underestimates Y in the concentration range of
$0 < X < 0.5$. A modification of the "regular" model was attempted and
this yielded an exchange function that is expressed as:

$$Y = \frac{X}{X + (1 - X)[K'' + c(1 - 2X)]} \qquad [45]$$

where K'' and c were found to be 8.0 and -4.0, respectively, in this
particular case. The modified exchange function is plotted as a solid

Table 5. The basic column and soil parameters for Experiment 5

Soil: Yolo fine sandy loam				
Items	Unit	Column		
		5-I	5-II	5-III
Flow velocity	cm/hr	7.3730	3.7319	5.3434
Dispersion coefficient	cm^2/hr	0.9498	0.2863	0.7967
Bulk density	g/cm^3	1.3060	1.3119	1.3023
Pore fraction		0.4696	0.4914	0.4600
Cation exchange capacity	me/g	0.2483	0.2501	0.2406
Total concentration	me/ml	0.1055	0.1049	0.1054
Column length	cm	23.0	23.1	23.0
Total time	hr	4.	10.	10.
Pore volume	ml	490.	515.	480.
Total input volume	ml	628.3	832.	1121.4
Total input volume	(pore volume)	1.2822	1.6155	2.3362

line in Figure 21. The modification improved the fit of the actual data points.

The similarity between Equation [45] and Equation [48] can be noted. Actually, this is a modification that changes the function from one with a constant separation factor to one that has a non-constant separation factor and, thus, an "irregular" type of exchange function.
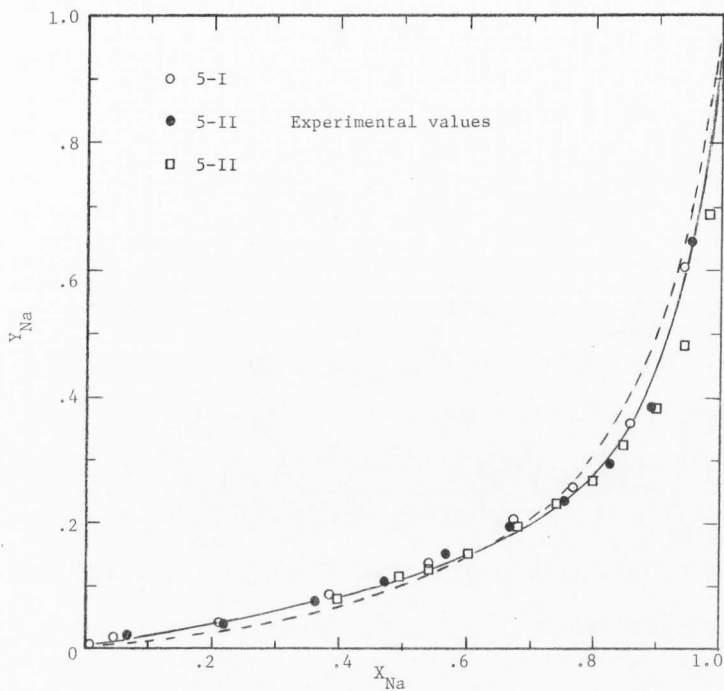
Figure 21. The Na→Ca exchange isotherm for Yolo fine sandy loam with data from three column experiments represented by spots, and two theoretical plots. The broken line is a plot from Equation [44] and the solid line is a plot from Equation [45].

The modified exchange function was used in solving the material balance equation. The solution of the latter equation in terms of $X(z,t)$ is presented in Figure 22a, b, and c along with the concentration profiles obtained from the three column experiments, respectively. The same data for $Y(z,t)$ are presented in Figure 23a, b, and c. The concentration profiles shown in Figure 22 and Figure 23 resemble qualitatively the results shown in Figure 11a and Figure 11b of Experiment 2.

Comparing the theoretically computed values of this experiment to those obtained from Experiment 2, the qualitative difference appears to be the rather sharp decrease of the concentration X at the front of the profiles. (Figure 22a,b.) This is attributed to the rather high average flow velocity combined with a very small dispersion coefficient found in these columns.

The sharp drop of concentration X at the profile front that was predicted by the theoretical computation did not show in the actual data obtained experimentally. Again, this can be due to the possibility that an actual equilibrium was not approached uniformly hence, the cation was allowed to travel further down the profile before it reached equilibrium with the exchanger phase and thus resulted in flatter profiles at the advancing front of the solute.

Although the deviation between the theoretical and experimental values appear at the front of the solution concentration profiles, it does not show to a significant extent in the profiles of the exchanger phase. This is due to the fact that in this concentration
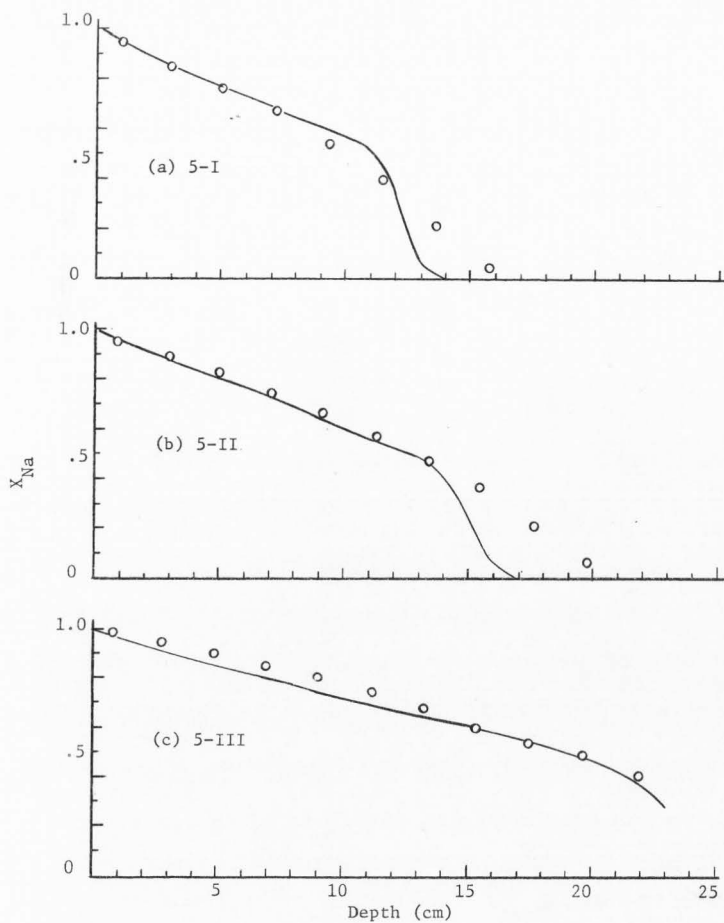
Figure 22. The cation concentration profiles $X(z,t)$ for the Na→Ca exchange for (a) column 5-I, (b) column 5-II, and (c) column 5-III. The solid lines are the computed values, the circles are the experimental values.
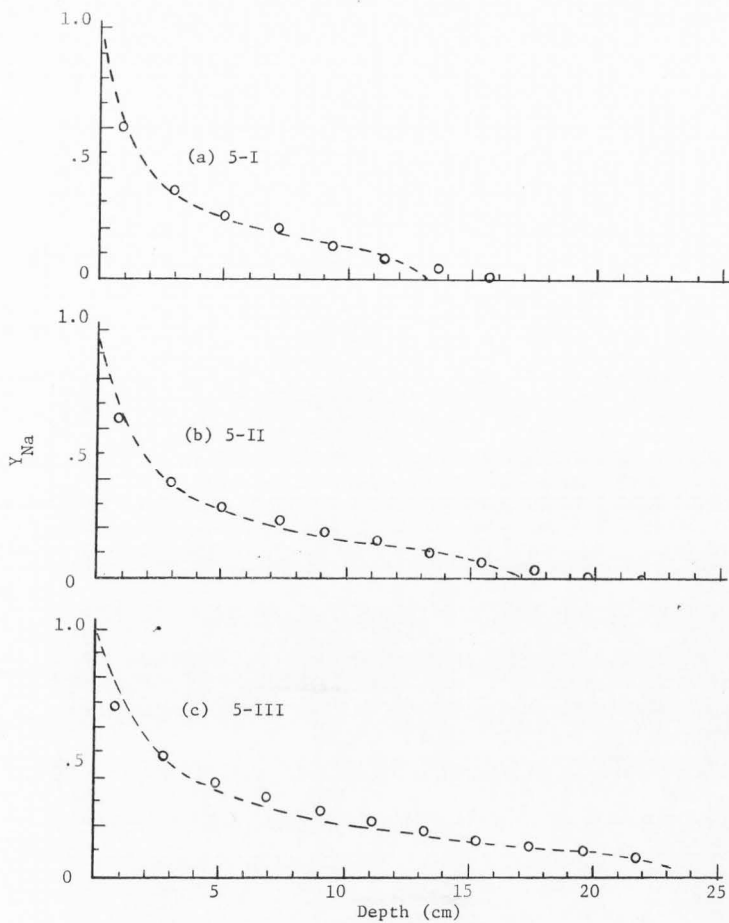
Figure 23. The cation concentration profiles Y(z,t) for the Na→Ca exchange for (a) column 5-I, (b) column 5-II, and (c) column 5-III. The dotted lines are the computed values, the circles are experimental values.

range, Y values are relatively small and change little with X. Thus, examination of Figure 23a, b, and c reveals a remarkably good agreement between the theoretical values and the experimental values.

In the column experiments, it was noticed that the flow velocity decreased with the amount of Na^+ solution introduced into the column. In Figure 24, the flow rate is plotted against time during the Na→Ca miscible displacement. It is noticed that Figure 24b shows a sharper decrease in the flow rate and it appears to be an exponential decrease while the flow rate in Figure 24a, and c show less intensive decrease with a nearly linear pattern. The actual reason for the difference in the patterns of the decrease in flow rate is not obvious. It was, however, noticed during the experiment that the top portion of column 5-II was disturbed and compacted before the miscible displacement was started.

In the theoretical computation, the overall average flow velocity was used. Those data presented in Figure 22 a, b, and c, and Figure 23 a, b, and c are from the computation with the average values of $\bar{V}$ and D. However, a computer experiment was also conducted to examine the effect of changing $\bar{V}$ with respect to the solution $X(z,t)$. The data for column 5-III was used and a computer program was developed to let $\bar{V}$ be a function of t while maintaining the $D/\bar{V}$ ratio as constant. The result is shown in Figure 25. It is seen that at the ten-hour period in which the experiment was conducted, the final result obtained from the use of average velocity is the same as the one using the actual decreasing velocity while maintaining the constant $D/\bar{V}$ ratio. However,
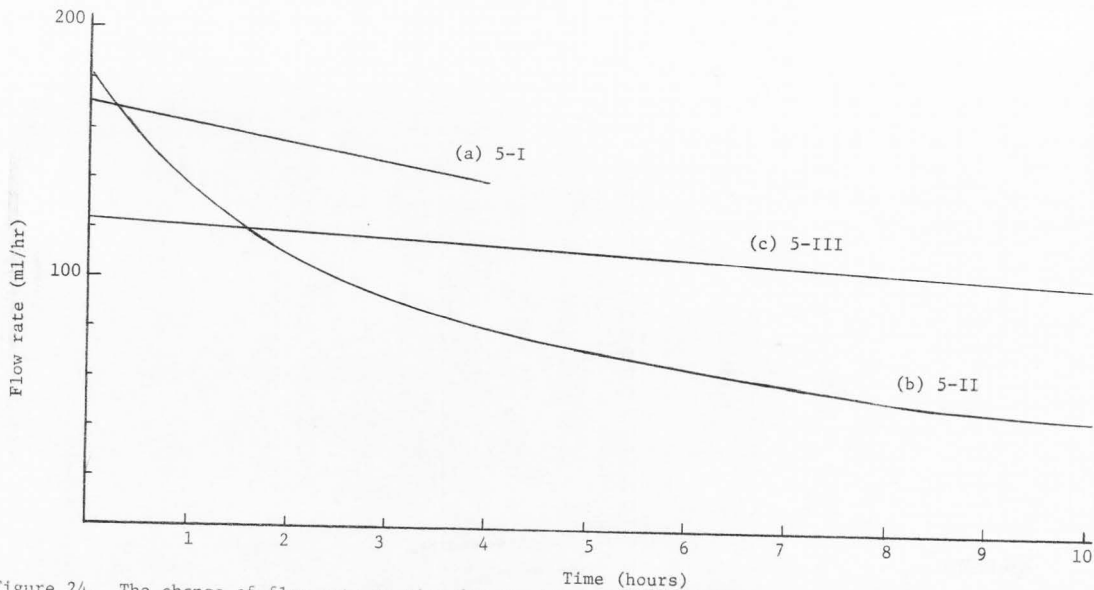
Figure 24. The change of flow rate *vs* time for the three column experiments (a) column 5-I, (b) column 5-II, and (c) column 5-III.
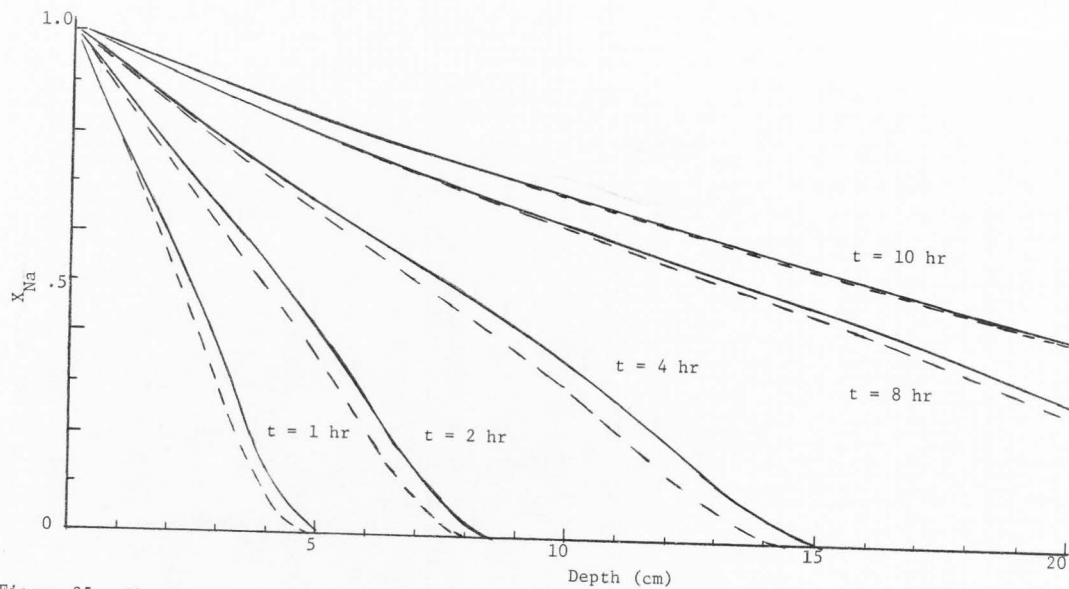
Figure 25. The cation concentration profiles $X(z,t)$ for column experiment 5-III. The broken lines show the profiles computed from using the average flow velocity. The solid lines show the profiles computed from using the actual flow velocity as a function of time.

during the intermediate time period, the profiles calculated from the decreasing velocity advances ahead of the ones from the average velocity. Thus, it can be concluded that use of average flow velocity is applicable only if the final result is desired. It would be in error to use the average flow velocity to predict the intermediate profiles.

This experiment shows a typical example of cation transport of the Type II isotherm which was discussed in Experiment 2.

In general, the model does describe the actual cation transport of this type. Some extent of discrepancy can be caused by the few things that were discussed earlier in Experiment 4. These are the possibilities of not having a complete equilibrium established uniformly in the column during the cation flow, the inadequate value of the dispersion coefficient, and those errors that could be caused by the chemical analysis and the numerical computation.

SUMMARY

A mathematical model was developed to predict the solution and the exchanger phase cation concentrations $X(z,t)$ and $Y(z,t)$, respectively in a one-dimensional cation solution displacement under a steady state flow condition.

The model consists of a parabolic partial differential equation and the initial and boundary conditions,

$$D \frac{\partial^2 X}{\partial z^2} - \bar{V} \frac{\partial X}{\partial z} = (1 + \frac{\rho Q}{\alpha C_o} f') \frac{\partial X}{\partial t} \qquad [40]$$

$$X(z,0) = 0 \qquad [41]$$

$$X(0,t) = 1.0 \qquad [42]$$

$$\frac{\partial X(L,t)}{\partial z} = 0 \qquad [43]$$

where f' is the slope of the cation exchange isotherm $f = f(X)$. The solutions, $X(z,t)$ and $Y(z,t)$, are obtained by using numerical methods conducted on a digital computer to solve the above equations.

Equation [40] is the material balance equation written in a partial differential form. The equation was derived from the mass conservation concept. It states that the change of the cation flux within a finite section of the soil column is equal to the rate of change of the cation concentration in solution phase plus the rate of change of the cation concentration in the exchanger phase. An assumption was made

that the cation concentration in the exchanger phase is in equilibrium with the cation concentration in the solution phase. Thus, the rate of change of the cation concentration in the exchanger phase was expressed by the slope of the cation exchange isotherm and the rate of change of concentration in the solution phase.

The parameters involved in Equation [40], D, $\bar{V}$, ρ, α, Q, and C_o, are determined experimentally.

The total study includes five experiments. Experiment 1 compared two numerical methods which were both capable of solving the mathematical problem in this study. It was found in this study that the two methods gave identical results while the explicit method was superior to the implicit one with a shorter computer run time and less computer storage requirement.

Experiment 2 involved a comparative study of the effect of the different characters of the exchange isotherms upon the behavior of the cation transport through the soil column. In this study, five different idealized isotherms were adopted in the solution of Equation [40] for $X(z,t)$ and $Y(z,t)$. It was shown that the character of the isotherm is reflected onto the cation concentration functions $X(z,t)$ and $Y(z,t)$. For an exchanging cation of strong separation factor, the resulted cation profiles are sharp with a strong "filtering effect." The function $Y(z,t)$ stays ahead of $X(z,t)$. For an exchanging cation of low separation factor, the opposite is true.

Experiment 3 was set up to compare two theoretical models, one proposed by Lapidus and Amundson (1952) with a linear isotherm, and the other proposed in this study with a non-linear isotherm. The Yolo fine

sandy loam was used for the column experiments. The experimentally determined isotherm was fitted into (a) a linear regression function, and (b) the Kielland exchange function (non-linear). The theoretically computed $X(z,t)$ and $Y(z,t)$ were compared. Though the two different theoretically fitted isotherms did not differ a great deal, the non-linear approach was found to be superior to the linear one.

Experiment 4 included the experimental verification of the model dealing with the Mg→Ca exchange. Two soils were used, namely the Nibley clay loam and the Hanford sandy loam. The agreement between the experimental value and the predicted value was good.

Experiment 5 involved the experimental verification of the model dealing with the Na→Ca exchange. Even with a fast flow rate, agreement between the theoretical prediction and the experimental value was satisfactory.

In both Experiments 4 and 5, some discrepancy between the theoretical and the experimental value of the concentration profiles was noted at the front ends of the profiles. Several possible factors could contribute to this discrepancy. Among them are the lack of complete equilibrium, the inadequate dispersion coefficient, and the experimental error from the chemical analysis and the numerical computation.

CONCLUSIONS AND APPLICATIONS

Conclusions

1. The cation exchange equilibria for the Mg→Ca reaction and the
   Na→Ca reaction studied do not show a constant separation fac-
   tor.

2. The cation exchange isotherm involving the Mg→Ca reaction are
   described successfully by a modified Kielland function.

3. The use of a dimensionless relative concentration as the depen-
   dent variables make the computation and the programming easier.

4. A comparison of the linear and the non-linear approach of
   handling the cation exchange function for the Mg→Ca exchange
   in Yolo fine sandy loam soil column yielded the conclusion
   that the non-linear approach is superior to the linear one.

5. The separation factor of the cation exchange revealed the
   characteristics of cation transport through the soil column.

6. The model proposed in this study including Equations [40]
   to [43] was found to be capable of predicting the cation
   transport process in the one-dimensional steady displacement
   through the soil column.

7. A slight discrepancy between the theoretically predicted
   value and the experimental value at the front of the cation
   profiles was attributed to the possible lack of the perfect
   equilibrium between the cation in solution phase and the one

in the exchanger phase, the inadequate dispersion coefficient
or the experimental error in the chemical analysis and compu-
tation. The first two factors may be the major causes.

8. The model proposed is capable of handling the problem involving
the variable flow velocity.

Applications

1. This model provides a working method that can handle all dif-
ferent types of cation exchange isotherms for predicting the
cation transport process involving miscible displacement.

2. This study provides a framework for solving problems that
involve water quality in respect to the cation composition
when different types of water are applied onto the soil
system.

3. This study also introduces a philosophy pertaining to the
solution of problems such as anion movement through the
adsorbent bed, and the other inorganic and organic chemical
movement through the adsorbent beds.

4. For chemical reactions occurring with a slow rate compared
to the fluid flow rate, a kinetic approach should replace
the equilibrium approach. Recommendations should be made
for this type of study since it covers a wide range of
problems in the adsorption of chemical onto the solid sur-
faces.

LITERATURE CITED

Ames, W. F. 1965. Nonlinear partial differential equations in engineering. Academic Press, New York.

Babcock, K. L. 1963. Theory of the chemical properties of soil colloidal systems. Hilgardia 34:496-523.

Barrer, R. M., and J. D. Falconer. 1956. Ion exchange in felspathoids as a solid-state reaction. Royal Soc. London Proc. A 236:227-249.

Berg, P. W., and J. L. McGregor. 1966. Elementary partial differential equations. Holden-Day, Inc., San Francisco.

Biggar, J. W., and D. R. Nielsen. 1963. Miscible displacement, V. exchange processes. Soil Sci. Soc. Amer. Proc. 27:623-627.

Bower, C. A., W. R. Gardner, and J. O. Goertzen. 1957. Dynamics of cation exchange in soil columns. Soil Sci. Soc. Amer. Proc. 21:20-24.

Brenner, H. 1962. The diffusion model of longitudinal mixing in beds of finite length: numerical values. Chem. Eng. Sci. 17: 229-243.

Carnahan, B., H. A. Luther, and J. O. Wilkes. 1969. Applied numerical methods. John Wiley and Sons, Inc., New York.

Clark, J. S., and R. C. Turner. 1965. Extraction of exchangeable cations and distribution constants for ion exchange. Soil Sci. Soc. Amer. Proc. 29:271-274.

Danckwerts, P. V. 1953. Continuous flow systems: distribution of residence times. Chem. Eng. Sci. 2:1-13.

DeVault, D. 1943. The theory of chromatography. J. Amer. Chem. Soc. 65:532-540.

Eriksson, E. 1952. Cation-exchange equilibria on clay minerals. Soil Sci. 74:103-113.

Helfferich, F. 1962. Ion exchange. McGraw-Hill Book Inc., New York.

Hiester, N. K., and T. Vermeulen. 1952. Saturation performance of ion-exchange and adsorption columns. Chem. Eng. Progress 48: 505-516.

Krishnamoorthy, C., and R. Overstreet. 1949. Theory of ion-exchange relationships. Soil Sci. 68:307-315.

Lapidus, L., and N. R. Amundson. 1952. Mathematics of adsorption in beds: VI. the effect of longitudinal diffusion in ion exchange and chromatographic columns. J. Phy. Chem. 56:984-988.

Nielsen, D. R., and J. W. Biggar. 1961. Miscible displacement in soils: I. experimental information. Soil Sci. Soc. Amer. Proc. 25:1-5.

Ogata, A. 1964. Mathematics of dispersion with linear adsorption isotherm. U. S. Geo. Survey Prof. Paper 411-H.

Peterson, F. F., J. Rhoades, M. Arca, and N. T. Coleman. 1965. Selective adsorption of magnesium ions by vermiculite. Soil Sci. Soc. Amer. Proc. 29:327-328.

Rible, J. M., and L. E. Davis. 1955. Ion exchange in soil columns. Soil Sci. 79:41-47.

Rifai, M. N. E., W. J. Kaufman, and D. K. Todd. 1956. Dispersion phenomena in laminar flow through porous media. Report No. 3, I. E. R. Series 90, Sani. Eng. Res. Lab., Univ. of Cal., Berkeley.

Thomas, H. C. 1944. Heterogeneous ion exchange in a flowing system. J. Amer. Chem. Soc. 66:1664-1666.

APPENDIXES

Appendix A

FORTRAN Programs

I. The FORTRAN program to solve the Equations [40] through [43], by
   the explicit method with a "Kielland" type exchange function.

```
C.................................................................
C
C    PURPOSE
C        TO SOLVE THE MATERIAL BALANCE EQUATION, WHICH IS THE INITIAL
C        BOUNDARY VALUE PROBLEM THAT GOVERNS THE CATION TRANSPORT
C        PROCESS IN THE STEADY DISPLACEMENT FLOW.
C
C    DESCRIPTION OF PARAMETERS
C        IDSET       NUMBER OF DATA SET
C        SIGN        DATA SET IDENTIFICATION AN ALPHANUMERIC
C                    ARRAY
C        D           DISPERSION COEFFICIENT
C        V           INTERSTITIAL FLOW VELOCITY
C        RO          BULK DENSITY
C        Q           CATION EXCHANGE CAPACITY
C        ALF         PORE FRACTION
C        CO          TOTAL CONCENTRATION
C        HZ          DEPTH INCREMENT
C        HT          TIME INCREMENT
C        IT          OUTPUT CONTROL NUMBER
C        IZ          OUTPUT CONTROL NUMBER
C        N           TOTAL NUMBER OF THE DEPTH INCREMENT
C        MT          TOTAL NUMBER OF THE TIME INCREMENT
C        C           CONSTANT IN KIELLAND FUNCTION
C        ALNK        CONSTANT IN KIELLAND FUNCTION
C        T           TIME
C        X           SOLUTION CONCENTRATION AN ARRAY
C        YOX         EXCHANGER CONCENTRATION  AN ARRAY
C
C    INPUT
C        SIGN
C        D,V,RO,Q,ALF,CO
C        HZ,HT,MT,N,IT,IZ
C        C,ALNK
C
C    OUTPUT
C        SIGN
C        D,V,RO,Q,ALF,CO
C        HZ,HT
C        C,ALNK
C        T,X(I)
C        YOX(I)
```

```
C
C     SUBROUTINE REQUIRED
C        EXFCN
C
C     METHOD
C        AN EXPLICIT METHOD DESCRIBED IN THE TEXT
C
C.................................................................................
C     MAIN PROGRAM
C
      DIMENSION X(100), Y(100), YOX(100), SIGN(11)
      IDSET = 2
      DO 10 ID = 1, IDSET
C
C     INPUT OF BASIC DATA
C
      READ(5,99) (SIGN(I), I = 1,11)
      WRITE(6,199)(SIGN(I), I = 1,11)
      READ(5,100) D,V,RO,Q,ALF,CO
      READ(5,101) HZ,HT,MT,N,IT,IZ
      WRITE(6,200) D,V,RO,Q,ALF,CO
      WRITE(6,201) HZ,HT
      NP1 = N + 1
      NM1 = N - 1
      DZ2 = D/(HZ*HZ)
      VZ = V/(2.*HZ)
      RQAC = (RO*Q)/(ALF*CO)
      READ(5,102)C, ALNK
      WRITE(6,202)C, ALNK
C
C     SET THE TOP BOUNDARY AND INITIAL CONDITIONS
C
      X(1) = 1.0
      DO 1 I = 2, NP1
    1 X(I) = 0.0
      KN = 0
      T = 0.0
C
C     BEGIN THE COMPUTATION OF X(I)
C
      DO 20 IIT = 1, MT
      DO 30 I = 2, N
      EOX = EXP(ALNK + C*(1. - 2.*X(I)))
      FOX = ((1. + 2.*C*X(I)*(1. - X(I)))*EOX)/((X(I) +
     &(1. - X(I))*EOX)**2)
      FT = (1. + RQAC*FOX)/HT
      Y(I) = ((DZ2 - VZ)*X(I + 1) - (2.*DZ2 - FT)*X(I) +
     &(DZ2 + VZ)*X(I - 1))/FT
   30 CONTINUE
```

```
C
C     EVALUATE THE BOTTOM BOUNDARY
C
      Y(NP1) = Y(NM1)
      DO 40 J = 2, NP1
   40 X(J) = Y(J)
      KN = KN + 1
      T = T + HT
      IF(KN.NE.IT) GO TO 20
C
C     OUTPUT X(I)
C
      WRITE(6,203) T, (X(I), I = 1, N, IZ)
C
C     COMPUTE YOX(I) IN SUBROUTINE EXFCN
C
      CALL EXFCN(X, C, ALNK, N, YOX)
C
C     OUTPUT YOX(I)
C
      WRITE(6,204) (YOX(I), I = 1, N)
      KN = 0
   20 CONTINUE
   10 CONTINUE
C
   99 FORMAT(11A4)
  100 FORMAT(6F10.4)
  101 FORMAT(2F10.4, 4I5)
  102 FORMAT(2F10.5)
  199 FORMAT(1H1, 10X, 11A4)
  200 FORMAT(1H1, 14X, 'DISPERSION COEFFICIENT', F15.6/15X,
     &'FLOW VELOCITY',F15.6/15X,'BULK DENSITY', F15.6/15X,
     &'EXCHANGE CAPACITY', F15.6/15X, 'PORE FRACTION', F15.6
     &/15X, 'TOTAL CONCENTRATION', F15.6)
  201 FORMAT (//14X, 'DEPTH INTERVAL',F15.6, 10X, 'TIME
     &INTERVAL', F15.6)
  202 FORMAT(1H1, 13X, 'CONSTANT C IS', F10.6, 'CONSTANT
     &LN K IS', F10.6//)
  203 FORMAT(1H , 14X, 'TIME IS', F10.2//(10F13.7))
  204 FORMAT(//(10F13.7))
      STOP
      END
```

```
C.............................................................
C
C    SUBROUTINE EXFCN
C
C    PURPOSE
C       TO EVALUATE Y(I) AS A FUNCTION OF X(I)
C
C    USAGE
C       CALL EXFCN(X, C, ALNK, N, YOX)
C
C.............................................................
C

         SUBROUTINE EXFCN(X, C, ALNK, N, YOX)
         DIMENSION X(100), YOX(100)
         DO 1 I = 1, N
       1 YOX(I) = X(I)/(X(I) + (1. - X(I))*EXP(ALNK + C*(1. -
        &2.*X(I))))
         RETURN
         END
```

II. The FORTRAN program to solve the Equations [40] through [43] by
    the implicit method with the predictor-corrector techniques.
    The exchange function is a Kielland type one.

```
C.................................................................,....
C
C     PURPOSE
C        TO SOLVE THE MATERIAL BALANCE EQUATION WHICH IS THE INITIAL
C        BOUNDARY VALUE PROBLEM GOVERNS THE CATION TRANSPORT PROCESS
C        IN A STEADY DISPLACEMENT FLOW
C
C     DESCRIPTION OF PARAMETERS
C        D             DISPERSION COEFFICIENT
C        V             FLOW VELOCITY
C        RO            BULK DENSITY
C        Q             CATION EXCHANGE CAPACITY
C        ALF           PORE FRACTION
C        CO            TOTAL CONCENTRATION
C        HZ            DEPTH INCREMENT
C        HT            TIME INCREMENT
C        T             TIME
C        MT            NUMBER OF TIME INCREMENT
C        N             NUMBER OF DEPTH INCREMENT
C        X             SOLUTION CONCENTRATION
C        FOX           EXCHANGER CONCENTRATION
C        C             CONSTANT IN EXCHANGE FUNCTION
C
C     INPUT
C        D, V, RO, Q, ALF, CO
C        HZ, HT, MT, N, IT, IZ
C        C
C
C     OUTPUT
C        D, V, RO, Q, ALF, CO
C        HZ, HT
C        C
C        SUM, KK
C        T, X(I)
C        FOX(I)
C
C     SUBROUTINE REQUIRED
C        TDMX
C
C     METHOD
C        THE IMPLICIT METHOD DESCRIBED IN THE TEXT
C
C.......................................................................
```

```
C     MAIN PROGRAM
      DIMENSION X(160), Y(160), Y1(160), B1(160), D1(160),
     &GOX(160), FOX(160)
  100 FORMAT(6F10.4)
  101 FORMAT(2F10.4, 4I5)
  102 FORMAT(F10.4)
  200 FORMAT(1H1, 14X, 'DISPERSION COEFFICIENT', F15.6/15X,
     &'FLOW VELOCITY',F15.6/15X, 'BULK DENSITY', F15.6/15X,
     &'EXCHANGE CAPACITY', F15.6/15X, 'PORE FRACTION', F15.6
     &/15X, 'TOTAL CONCENTRATION', F15.6)
  201 FORMAT(//14X, 'DEPTH INTERVAL', F15.6, 10X, 'TIME', F15.6)
  202 FORMAT(1H1, 13X, 'EXCHANGE CONSTANT IS', F10.4//)
  203 FORMAT(1H , 14X, 'TIME IS', F10.2//(10F13.7))
  204 FORMAT(//(10F13.7))
  205 FORMAT(//'SUM = ', E15.7, 'NO OF ITERATION = ', I5)
C
C     INPUT BASIC DATA
C
      READ(5,100) D, V, RO, Q, ALF, CO
      READ(5,101) HZ, HT, MT, N, IT, IZ
      WRITE(6,200) D, V, RO, Q, ALF, CO
      WRITE(6,201) HZ, HT
      EPSI = 0.0001
      NP1 = N + 1
      NM1 = N - 1
      A1 = D*HT
      VZT = V*HZ*HT
      C1 = A1 - VZT
      BO = 2.*A1 - VZT
      HZZ = HZ*HZ
      RQAC = (RO*Q)/(ALF*CO)
      READ(5,102) C
      WRITE(6,202) C
C
C     SET THE BOUNDARY AND THE INITIAL CONDITIONS
C
      X(1) = 1.0
      Y(1) = 1.0
      Y1(1) = 1.0
      DO 1 I = 2,NP1
      X(I) = 0.0
      Y(I) = 0.0
    1 Y1(I) = 0.0
      KN = 0
      T = 0.0
C
C     BEGIN THE COMPUTATION
```

```
C
      DO 20 IIT = 1, MT
      KK = 0
    3 DO 2 J = 1, NP1
      EOX = EXP(C*(1. - 2.*Y(J)))
      FPOX = ((1. + 2.*C*Y(J)*(1. - Y(J)))*EOX)/((Y(J) +
     &(1. - Y(J))*EOX**2)
      GOX(J) = (1. + RQAC*FPOX)
      B1(J) = -(BO + GOX(J)*HZZ)
    2 D1(J) = -GOX(J)*HZZ*X(J)
C
C     SOLVE THE TRIDIAGONAL MATRIX BY SUBROUTINE TDMX
C
      CALL TDMX(A1, B1, C1, D1, Y1, N)
      SUM = 0.0
      DO 5 I = 2, NP1
      DIF = Y1(I) - Y(I)
    5 SUM = SUM + ABS(DIF)
C
C     TEST THE CONVERGENCY
C
      IF(SUM.LT.EPSI.OR.KK.GT.10) GO TO 11
      DO 6 I = 2, NP1
    6 Y(I) = Y1(I)
      KK = KK + 1
      GO TO 3
   11 T = T + HT
      DO 8 I = 2, NP1
      X(I) = Y1(I)
    8 Y(I) = Y1(I)
      KN = KN + 1
      IF (KN.NE.IT) GO TO 20
C
C     OUTPUT OF THE ANSWER
C
      WRITE(6,205) SUM, KK
      WRITE(6,203) T, (X(I), I = 1, NP1, IZ)
      DO 12 I = 1,NP1, IZ
   12 FOX(I) = X(I)/(X(I) + (1. - X(I))*EXP(C*(1. - 2.*
     &X(I))))
      WRITE(6,204)(FOX(I), I = 1, NP1, IZ)
      KN = 0
   20 CONTINUE
      STOP
      END
```

```
C.........................................................................
C
C     SUBROUTINE TDMX
C
C     PURPOSE
C        TO SOLVE THE TRIDIAGONAL MATRIX
C
      DESCRIPTION OF PARAMETERS
C        AT, BT, CT ELEMENTS OF THE COEFFICIENT MATRIX
C        DT       THE RIGHT HAND SIDE VECTOR
C
C     METHOD
C        FIRST, THE ELIMINATION OF THE LOWER DIAGONAL OF THE
C        MATRIX.  THEN THE X(I) ARE SOLVED BY BACK SUBSTITUTION
C
C     USAGE
C        CALL TDMX(A1, B1, C1, D1, Y1, N)
C
C.........................................................................

      SUBROUTINE TDMX(AT, BT, CT, DT, X, N)
      DIMENSION BT(160), X(160), CCT(160), DDT(160)
      CCT(2) = CT/BT(2)
      DDT(2) = (DT(2) - AT)/BT(2)
      NP1 = N + 1
      DO 100 I = 3, N
      TEMPO = (BT(I) - AT*CCT(I - 1))
      CCT(I) = CT/TEMPO
      DDT(I) = (DT(I) - AT*DDT(I - 1))/TEMPO
  100 CONTINUE
      DDT(NP1) = (DT(NP1) - AT*DDT(N))/(BT(NP1) + CT - AT*
     &CCT(N))
      X(NP1) = DDT(NP1)
      J = NP1
   10 J = J - 1
      X(J) = DDT(J) - CCT(J)*X(J + 1)
      IF(J.NE.2) GO TO 10
      RETURN
      END
```

III. The FORTRAN program to solve the Equations [40] through [43]
     with a linear exchange isotherm in Experiment 3.

```
C.................................................................
C
C    PURPOSE
C        TO SOLVE THE MATERIAL BALANCE EQUATION THAT GOVERNS
C        THE CATION TRANSPORT WITH A LINEAR CATION EXCHANGE
C        FUNCTION
C
C    DESCRIPTION OF PARAMETERS
C        D          DISPERSION COEFFICIENT
C        V          FLOW VELOCITY
C        RO         BULK DENSITY
C        Q          EXCHANGE CAPACITY
C        ALF        PORE FRACTION
C        CO         TOTAL CONCENTRATION
C        HZ         DEPTH INCREMENT
C        HT         TIME INCREMENT
C        MT         NUMBER OF TIME INCREMENT
C        N          NUMBER OF THE DEPTH INCREMENT
C        SLOPE      THE CONSTANT OF THE EXCHANGE FUNCTION
C        AINCP      THE CONSTANT OF THE EXCHANGE FUNCTION
C        X          SOLUTION CONCENTRATION
C        T          TIME
C        FOX        EXCHANGER CONCENTRATION
C
C    INPUT
C        D, V, RO, Q, ALF, CO
C        HZ, HT, MT, N, IT, IZ
C        SLOPE, AINCP
C
C    OUTPUT
C        D, V, RO, Q, ALF, CO
C        HZ, HT
C        SLOPE, AINCP
C        T, X(I)
C        FOX(I)
C
C    METHOD
C        THE EXPLICIT METHOD DESCRIBED IN THE TEXT WITH A LINEAR
C        EXCHANGE FUNCTION
C
C.................................................................

C    MAIN PROGRAM
         DIMENSION X(100), Y(100), FOX(100)
C
C    INPUT BASIC DATA
```

```
C
          READ(5,100) D, V, RO, Q, ALF, CO
          READ(5,101) HZ, HT, MT, N, IT, IZ
          WRITE(6,200) D, V, RO, Q, ALF, CO
          WRITE(6,201) HZ, HT
          READ(5,102) SLOPE, AINCP
          WRITE(6,204) SLOPE, AINCP
          NP1 = N + 1
          NM1 = N - 1
          DZ2 = D/(HZ*HZ)
          VZ = V/(2.*HZ)
          RQAC = (RO*Q*SLOPE)/(ALF*CO)
          FT = (1. + RQAC)/HT
C
C     SET THE BOUNDARY AND THE INITIAL CONDITIONS
C
          X(1) = 1.0
          DO 1 I = 2, NP1
        1 X(I) = 0.0
          KN = 0
          T = 0.0
C
C     BEGIN THE COMPUTATION OF X(I)
C
          DO 20 IIT = 1, MT
          DO 30 I = 2, N
          Y(I) = ((DZ2 - VZ)*X(I + 1) - (2.*DZ2 - FT)*X(I) +
         &(DZ2 + VZ)*X(I - 1))/FT
       30 CONTINUE
          Y(NP1) = Y(NM1)
          DO 40 J = 2, NP1
       40 X(J) = Y(J)
          KN = KN + 1
          T = T + HT
          IF(KN.NE.IT) GO TO 20
C
C     OUTPUT OF X(I) AND FOX(I)
C
          WRITE(6,203) T, (X(I), I = 1, N, IZ)
          DO 50 I = 1, N
       50 FOX(I) = AINCP + X(I)*SLOPE
          WRITE(6,205) (FOX(I), I = 1, N, IZ)
          KN = 0
       20 CONTINUE
      100 FORMAT(6F10.4)
      101 FORMAT(2F10.4,4I5)
      102 FORMAT(2F10.5)
      200 FORMAT(1H1, 14X, 'DISPERSION COEFFICIENT', F15.6/15X,
         &'FLOW VELOCITY', F15.6/15X, 'BULK DENSITY', F15.6/
```

```
      &15X, 'EXCHANGE CAPACITY', F15.6/15X, 'PORE FRACTION',
      &F15.6/15X, 'TOTAL CONCENTRATION', F15.6)
  201 FORMAT(//14X, 'DEPTH INTERVAL', F15.6, 10X, 'TIME
      &INTERVAL', F15.6)
  203 FORMAT(1H , 14X, 'TIME IS', F10.2//(10F13.7))
  204 FORMAT(1H1, 'SLOPE OF THE EXCHANGE FUNCTION IS', F10.6,
      &'     INTERCEPT IS', F10.6)
  205 FORMAT(//(10F13.7))
      STOP
      END
```

Appendix B

Derivation of Equation

The derivation of Equation [51] from Equation [50] was done by Rifai et al. (1956). The details of the development will be treated here for reference.

Equation [50] is restated here setting z = L.

$$\frac{C}{C_o} = \frac{1}{2} \left[1 - erf \left(\frac{L - \bar{V}t}{2\sqrt{Dt}} \right) \right]$$ [50]

This equation is first altered into a form where the independent variable V is put in place of t, applying the relationship

$$\frac{J}{V_o} = \frac{\bar{V}}{L}$$

$$\bar{V} = \frac{J \cdot L}{V_o}$$ [c-1]

$$\bar{V}t = Jt \frac{L}{V_o} = \frac{V}{V_o} L$$ [c-2]

$$t = \frac{VL}{V_o \bar{V}} = \frac{V}{J}$$

where J is the flux. Equation [50] is now transformed into

$$\frac{C}{C_o} = \frac{1}{2} \left[1 - erf \left(\frac{L}{2V_o} \sqrt{\frac{J}{D}} \frac{V_o - V}{\sqrt{V}} \right) \right]$$

$$= \frac{1}{2} \left[1 - erf \left(\frac{1}{2} \sqrt{\frac{VL}{DV_o}} \frac{V_o - V}{\sqrt{V}} \right) \right]$$ [c-3]

The error function in Equation [c-3] is now written into an infinite integral

$$\frac{C}{C_o} = \frac{1}{2} \left[1 - \frac{2}{\sqrt{\pi}} \int e^{-\alpha^2} d\alpha \right] \qquad [c-4]$$

where

$$\alpha = \frac{1}{2} \sqrt{\frac{\overline{V}L}{DV_o}} \frac{V_o - V}{\sqrt{V}}$$

Recalling that our objective here is to find an expression for D in terms of the measurable quantity from the characteristics of the whole breakthrough curve. We now differentiate Equation [c-4] with respect to the effluent volume V at $V = V_o$.

$$\frac{d(C/C_o)}{dV} = \frac{d}{dV} \left[\frac{1}{2} \left(1 - \frac{2}{\sqrt{\pi}} \int e^{-\alpha^2} d\alpha \right] \right.$$

$$= \frac{1}{4\sqrt{\pi}} e^{-\alpha^2} \sqrt{\frac{\overline{V}L}{DV_o}} \frac{1}{\sqrt{V}} \left(\frac{V + V_o}{V} \right) \qquad [c-5]$$

Defining

$$S_o = \frac{d(C/C_o)}{dV} \bigg|_{V = V_o}$$

where S_o is the slope of the BTC at $V = V_o$,

$$S_o = \frac{1}{4\sqrt{\pi}} \sqrt{\frac{\overline{V} L}{D}} \frac{1}{\sqrt{V_o}} \frac{V_o + V_o}{V_o} \qquad [c-6]$$

Thus,

$$S_o = \frac{1}{2\sqrt{\pi}} \sqrt{\frac{\bar{V} L}{D}} \; \frac{1}{V_o} \qquad [c-7]$$

or

$$\frac{D}{\bar{V}} = \frac{L}{4\pi \, S_o^{\,2} V_o^{\,2}} \qquad [51]$$

This completes the derivation of Equation [51].

Appendix C

Tables

Table 6. Chloride breakthrough curve data for Experiment 3

Soil: Yolo fine sandy loam			

Column 3-I		Column 3-III	
Effluent Volume	C/C_o	Effluent Volume	C/C_o
(ml)		(ml)	
5.1	.005	97.9	0.003
96.9	.003	200.9	0.005
147.9	.005	252.4	0.005
198.9	.005	303.9	0.005
249.9	.006	355.4	0.005
300.9	.008	406.9	0.083
351.9	.052	427.5	0.170
402.9	.243	448.1	0.286
423.3	.349	468.7	0.419
443.7	.445	489.3	0.576
464.1	.538	509.9	0.709
484.5	.613	561.4	0.922
504.9	.693	612.9	0.980
555.9	.809	664.4	1.003
606.9	.889	715.9	0.997
657.9	.943	818.9	1.005
708.9	.969	921.9	1.003
759.9	.990		
810.9	.985		

C_o = 0.09675 me/ml C_o = 0.09975 me/ml

Table 7.   Chloride breakthrough curve data for Experiment 4

Soil: Nibley clay loam

Column 4-I		Column 4-II		Column 4-III	
Effluent Volume	C/C_o	Effluent Volume	C/C_o	Effluent Volume	C/C_o
(ml)		(ml)		(ml)	
5.1	0.00	15.3	0.00	5.20	0.005
96.9	0.00	96.9	0.00	97.90	0.005
198.9	0.00	198.9	0.00	200.9	0.00
				252.4	0.00
249.9	.041	249.9	0.003	303.9	0.012
300.9	0.145	300.9	0.031	355.4	0.060
382.5	0.237	321.3	0.062	386.3	0.119
				406.9	0.171
413.1	0.323	341.7	0.106	427.5	0.233
443.7	0.416	362.1	0.158	448.1	0.305
				468.7	0.382
459.0	0.457	382.5	0.224	489.3	0.452
474.3	0.501	402.9	0.293	509.9	0.528
494.7	0.552	423.3	0.355	530.5	0.588
				551.1	0.658
525.3	0.609	443.7	0.420	571.7	0.709
586.5	0.699	464.1	0.472	592.3	0.752
		484.5	0.526	612.9	0.802
617.1	0.751	504.9	0.578	664.4	0.878
657.9	0.813	525.3	0.617	715.9	0.908
		566.1	0.692	767.4	0.958
708.9	0.852	606.9	0.749	818.9	0.970
759.9	0.893	647.7	0.803	870.4	0.985
861.9	0.952	688.5	.8472	973.4	0.995
963.9	0.9781	739.5	.9041		
C_o = 0.09675 me/ml		C_o = 0.0965 me/ml		C_o = 0.0995 me/ml	

Table 8. Chloride breakthrough curve data for Experiment 4

Soil: Hanford sandy loam					
Column 4-I		Column 4-II		Column 4-III	
Effluent Volume	C/C_o	Effluent Volume	C/C_o	Effluent Volume	C/C_o
(ml)		(ml)		(ml)	
249.9	0.0	198.9	.003	97.8	.001
300.9	0.015	249.9	.005	149.4	0.00
331.5	0.113	300.9	.005	200.9	0.00
351.9	0.229	331.5	0.065	252.4	0.00
372.3	0.369	351.9	0.182	303.9	0.002
382.5	0.448	372.3	0.347	334.8	0.058
392.7	0.818	382.5	0.430	355.4	0.190
402.7	0.572	392.7	0.505	365.7	0.289
413.1	0.635	402.9	0.573	375.9	0.390
433.5	0.732	413.1	0.641	386.4	.484
453.9	0.793	433.5	0.735	396.6	0.583
484.5	0.857	453.9	0.805	406.9	0.648
525.3	0.928	484.5	0.886	417.2	0.704
555.9	0.956	525.3	0.937	427.5	0.747
606.9	0.985	555.9	0.966	448.1	0.827
657.9	0.989	606.9	0.985	468.7	0.884
708.9	1.009	557.9	0.996	489.3	0.908
759.9	1.000	698.7	1.002	530.5	0.986
				612.9	1.00
C_o = 0.0953 me/ml		C_o = 0.0958 me/ml		C_o = 0.1036 me/ml	

Table 9. Chloride breakthrough curve data for Experiment 5

Soil: Yolo fine sandy loam					
Column 5-I		Column 5-II		Column 5-III	
Effluent Volume	C/C_o	Effluent Volume	C/C_o	Effluent Volume	C/C_o
(ml)		(ml)		(ml)	
5.2	.995	5.2	.960	5.2	.940
97.9	1.005	97.9	1.000	87.9	1.000
200.9	.995	200.9	1.000	200.85	.995
252.4	.990	252.4	.995	252.4	.995
303.9	1.000	303.9	1.025	303.9	1.010
355.4	1.000	355.4	1.000	355.4	1.005
406.9	.990	406.9	.985	406.9	.965
437.8	.890	427.5	1.020	427.5	.870
458.4	.750	468.7	.884	448.1	.710
479.0	0.580	489.3	.744	468.7	.555
499.6	.410	509.9	.558	489.3	.405
509.9	.340	530.5	.342	509.9	.275
530.5	.230	551.1	.181	530.5	.175
561.4	.140	602.6	0.025	561.4	.082
612.9	.075	664.4	0.00	612.9	.025
				715.9	.005
C_o = 0.100 me/ml		C_o = 0.0995 me/ml		C_o = 0.100 me/ml	

Table 10. The cation concentration profiles of Mg^{++} determined from column experiment 3-I, Yolo fine sandy loam

Depth (cm)	C_o (me/ml)	Q (me/20g)	X_{mg}	Y_{mg}
1.2	.1111	5.266	.9774	.9526
3.4	.1085	5.199	.9020	.8620
5.5	.1056	5.087	.6387	.6566
7.6	.1068	4.890	.2746	.2984
9.7	.1028	4.849	.0638	.1123
11.8	.1027	4.821	.0139	.0490
13.9	.1029	4.873	.0099	.0400
16.0	.1098	4.834	.0149	.0404
18.2	.0981	4.894	.0125	.0440
20.3	.1040	4.834	.0148	.0425
23.2	.1057	4.854	.0243	.0592

Table 11. The cation concentration profiles of Mg^{++} determined from column experiment 3-II, Yolo fine sandy loam

Depth (cm)	C_o (me/ml)	Q (me/20g)	X_{mg}	Y_{mg}
1.5	.1053	5.307	.9881	.9646
3.6	.1061	5.298	.9788	.9410
5.7	.1063	5.352	.9636	.9124
7.8	.1052	5.312	.9228	.8611
9.9	.1044	5.299	.8387	.7759
12.0	.1039	5.205	.7022	.6517
14.1	.1038	5.059	.4772	.4835
16.2	.1016	4.825	.2631	.2875
18.3	.0987	4.674	.1395	.1495
20.4	.1018	4.596	.0242	.0738
23.2	.1015	4.591	.0202	.0402

Table 12. The cation concentration profiles of Mg^{++} determined from column experiment 3-III, Yolo fine sandy loam

Depth (cm)	C_o (me/ml)	Q (me/20g)	X_{mg}	Y_{mg}
1.4	.1092	5.578	.9942	.9731
3.7	.1070	5.542	.9912	.9572
5.8	.1047	5.700	.9821	.9343
7.9	.1078	5.557	.9652	.9101
10.0	.1066	5.663	.9297	.8567
12.1	.1050	5.536	.8455	.7835
14.2	.1097	5.336	.7497	.6935
16.3	.1049	5.383	.6430	.6035
18.4	.1066	5.366	.5786	.5057
20.5	.1049	5.331	.3996	.4088
22.6	.1066	5.327	.3703	.2971

Table 13. The cation concentration profiles of Mg^{++} determined from column experiment 4-I, Nibley clay loam

Depth (cm)	C_o (me/ml)	Q (me/20g)	X_{mg}	Y_{mg}
.6	.1155	6.378	.9168	.7897
2.6	.1143	5.838	.5632	.4102
4.8	.1088	5.716	.2777	.2285
6.9	.1072	5.502	.0806	.1158
9.0	.1065	5.321	.0039	.0329
11.1	.1065	5.072	.0039	.0223
13.2	.1052	5.103	.0039	.0221
15.3	.1027	4.927	.0039	.0189
17.5	.1040	4.947	.0039	.0166
19.6	.1021	4.916	.0039	.0167
22.3	.1033	4.854	.0039	.0169

Table 14. The cation concentration profiles of Mg^{++} determined from column experiment 4-II, Nibley clay loam

Depth (cm)	C_o (me/ml)	Q (me/20g)	X_{mg}	Y_{mg}
.6	.1229	6.030	.9929	.9070
2.6	.1175	6.687	.9713	.7378
4.8	.1149	6.121	.8025	.6515
6.9	.1099	5.982	.7150	.5465
9.0	.1112	5.864	.5288	.4628
11.1	.1078	5.655	.3336	.3381
13.2	.1087	5.517	.1626	.2199
15.3	.1059	5.237	.0699	.0472
17.5	.1060	5.286	.0175	.0972
19.6	.1064	5.112	.0095	.0201
22.3	.1052	5.103	.0098	.0161

Table 15. The cation concentration profiles of Mg^{++} determined from column experiment 4-III, Nibley clay loam

Depth (cm)	C_o (me/ml)	Q (me/20g)	X_{mg}	Y_{mg}
1.2	.1067	5.446	.9787	.9059
3.5	.1075	5.618	.9258	.8124
5.7	.1053	5.724	.9135	.7362
7.8	.1162	5.966	.8529	.6753
9.9	.1143	6.134	.7408	.6100
12.0	.1119	6.378	.6539	.5222
14.1	.1176	6.511	.4964	.4357
16.2	.1045	6.499	.3187	.3384
18.3	.1102	6.616	.2611	.2423
20.4	.1149	6.558	.1324	.1661
22.5	.1132	6.313	.029	.0977

Table 16. The cation concentration profiles of Mg^{++} determined from column experiment 4-I, Hanford sandy loam

Depth (cm)	C_o (me/ml)	Q (me/25g)	X_{mg}	Y_{mg}
.8	.1091	1.533	.9900	.9290
2.6	.1084	1.472	.9390	.7950
4.7	.1098	1.400	.7120	.5890
6.9	.1069	1.373	.2350	.2450
9.0	.1047	1.328	.0100	.0020
11.1	.1032	1.350	.00	.00
13.2	.1018	1.374	.00	.00
15.4	.1006	1.344	.00	.00
17.5	.0975	1.364	.00	.00
19.6	.0968	1.354	.00	.00
22.8	.0968	1.320	.00	.00

Table 17. The cation concentration profiles of Mg^{++} determined from column experiment 4-II, Hanford sandy loam

Depth (cm)	C_o (me/ml)	Q (me/25g)	X_{mg}	Y_{mg}
1.1	.1087	1.598	.9950	.9590
3.4	.1099	1.554	.9850	.9080
5.5	.1099	1.480	.9550	.8480
7.6	.1084	1.474	.8950	.7500
9.7	.1095	1.479	.7580	.6260
11.9	.1113	1.408	.5910	.4680
14.0	.1061	1.387	.2220	.2430
16.1	.1039	1.344	.0198	.0610
18.2	.1018	1.350	.00	.00
20.4	.1018	1.363	.00	.00
23.2	.1057	1.363	.00	.00

Table 18. The cation concentration profiles of Mg^{++} determined from column experiment 4-III, Hanford sandy loam

Depth (cm)	C_o (me/ml)	Q (me/25g)	X_{mg}	Y_{mg}
1.0	.1162	1.625	.9978	.9539
2.9	.1072	1.592	.9977	.9452
5.0	.1073	1.568	.9768	.9125
7.1	.1094	1.573	.9772	.8731
9.2	.1086	1.589	.9541	.8257
11.3	.1062	1.581	.9178	.7696
13.4	.1059	1.589	.8539	.6908
15.5	.1046	1.578	.7544	.5810
17.6	.1050	1.531	.6342	.4915
19.7	.1054	1.552	.5266	.4134
21.9	.1080	1.509	.4340	.3352

Table 19. The cation concentration profiles of Na^+ determined from column experiment 5-I, Yolo fine sandy loam

Depth (cm)	C_o (me/ml)	Q (me/20g)	X_{Na}	Y_{Na}
1.0	.1095	5.008	.9430	.6014
3.0	.1063	5.106	.8591	.3598
5.1	.1080	5.036	.7690	.2569
7.2	.1067	5.050	.6726	.2045
9.4	.1075	5.024	.5403	.1385
11.5	.1055	4.926	.3853	.0882
13.6	.1043	4.869	.2105	.0468
15.7	.1041	4.901	.0459	.0199
17.8	.1034	4.920	.0105	.0110
20.0	.1034	4.920	.0105	.0110
22.0	.1014	4.864	.0085	.0022

Table 20. The cation concentration profiles of Na^+ determined from column experiment 5-II, Yolo fine sandy loam

Depth (cm)	C_o (me/ml)	Q (me/20g)	X_{Na}	Y_{Na}
.9	.1126	5.071	.9556	.6432
3.0	.1103	5.051	.8913	.3874
5.0	.1065	5.095	.8267	.2923
7.1	.1041	4.968	.7580	.2341
9.2	.1056	5.011	.6692	.1909
11.3	.1075	5.015	.5705	.1517
13.4	.1038	4.972	.4713	.1093
15.5	.1023	4.984	.3612	.0763
17.7	.1018	4.896	.2157	.0444
19.8	.1008	4.974	.0690	.0218
22.0	.0984	4.982	.0110	.0109

Table 21. The cation concentration profiles of Na^+ determined from column experiment 5-III, Yolo fine sandy loam

Depth (cm)	C_o (me/ml)	Q (me/20g)	X_{Na}	Y_{Na}
.9	.1103	5.017	.9819	.6892
2.8	.1067	4.950	.9415	.4833
4.9	.1048	4.938	.9048	.3810
7.0	.1083	4.883	.8479	.3229
9.1	.1004	4.837	.8013	.2675
11.2	.1028	4.768	.7450	.2281
13.3	.1055	4.946	.6806	.1979
15.4	.1056	4.685	.6054	.1532
17.5	.1044	4.690	.5414	.1275
19.7	.1063	4.661	.4952	.1167
21.9	.1048	4.572	.4047	.0832

Table 22. The concentration function X(z,t) computed for Experiment
2 for Type I isotherm

Depth	Time (hours)					
	10	20	40	60	80	100
(cm)						
0	1.0000	1.0000	1.0000	1.0000	1.0000	1.0000
1	.8650	.9744	.9987	.9999	1.0000	1.0000
2	.5477	.9116	.9955	.9998	1.0000	1.0000
3	.0436	.7664	.9880	.9994	1.0000	1.0000
4	.0003	.4531	.9707	.9984	.9999	1.0000
5	.0000	.0314	.9314	.9963	.9998	1.0000
6		.0003	.8435	.9914	.9995	1.0000
7		.0000	.6515	.9805	.9989	.9999
8			.2737	.9559	.9976	.9999
9			.0062	.9009	.9946	.9997
10			.0001	.7793	.9877	.9993
11			.0000	.5219	.9724	.9985
12				.0806	.9380	.9966
13				.0010	.8614	.9924
14				.0000	.6946	.9828
15					.3542	.9614
16					.0139	.9134
17					.0001	.8074
18					.0000	.5794
19						.1485
20						.0021
21						.0000
22						
23						
24						
25						
26						
27						
28						
29						
30						

Table 23. The concentration function $X(z,t)$ computed for Experiment 2 for Type II isotherm

Depth	Time (hours)					
	10	20	40	60	80	100
(cm)						
0	1.0000	1.0000	1.0000	1.0000	1.0000	1.0000
1	.8948	.9431	.9731	.9841	.9896	.9928
2	.7976	.8842	.9404	.9625	.9743	.9815
3	.7094	.8294	.9076	.9394	.9569	.9679
4	.6272	.7781	.8762	.9164	.9388	.9533
5	.5494	.7296	.8464	.8941	.9210	.9385
6	.4752	.6832	.8179	.8726	.9036	.9239
7	.4046	.6384	.7906	.8520	.8868	.9096
8	.3379	.5947	.7642	.8321	.8705	.8956
9	.2759	.5520	.7386	.8129	.8547	.8821
10	.2194	.5100	.7136	.7942	.8394	.8690
11	.1691	.4689	.6892	.7761	.8245	.8562
12	.1260	.4285	.6652	.7583	.8099	.8437
13	.0902	.3889	.6416	.7409	.7958	.8316
14	.0618	.3503	.6183	.7238	.7819	.8197
15	.0404	.3128	.5952	.7070	.7683	.8080
16	.0251	.2765	.5724	.6905	.7549	.7966
17	.0147	.2418	.5497	.6741	.7418	.7854
18	.0081	.2089	.5271	.6579	.7288	.7743
19	.0042	.1781	.5047	.6419	.7160	.7635
20	.0020	.1496	.4824	.6260	.7033	.7527
21	.0009	.1237	.4602	.6102	.6908	.7422
22	.0004	.1004	.4381	.5945	.6784	.7317
23	.0002	.0799	.4161	.5789	.6661	.7214
24	.0001	.0624	.3943	.5634	.6539	.7111
25	.0000	.0476	.3726	.5480	.6418	.7010
26		.0355	.3513	.5327	.6299	.6910
27		.0258	.3304	.5177	.6183	.6813
28		.0184	.3108	.5035	.6072	.6722
29		.0132	.2941	.4915	.5979	.6644
30		.0108	.2857	.4853	.5931	.6604

Table 24. The concentration function X(z,t) computed for Experiment 2 for Type III isotherm

Depth	Time (hours)					
	10	20	40	60	80	100
(cm)						
0	1.0000	1.0000	1.0000	1.0000	1.0000	1.0000
1	.8561	.9528	.9912	.9978	.9994	.9998
2	.6299	.8643	.9729	.9932	.9981	.9994
3	.3851	.7336	.9409	.9846	.9956	.9986
4	.1919	.5740	.8913	.9700	.9911	.9973
5	.0772	.4091	.8220	.9474	.9839	.9949
6	.0250	.2635	.7338	.9145	.9726	.9911
7	.0065	.1524	.6304	.8699	.9560	.9851
8	.0014	.0789	.5189	.8126	.9327	.9764
9	.0002	.0365	.4076	.7432	.9016	.9640
10	.0000	.0151	.3045	.6634	.8617	.9469
11		.0055	.2158	.5765	.8125	.9243
12		.0018	.1448	.4864	.7544	.8952
13		.0005	.0918	.3977	.6883	.8593
14		.0001	.0550	.3146	.6160	.8160
15		.0000	.0311	.2403	.5399	.7657
16			.0166	.1770	.4627	.7088
17			.0083	.1257	.3872	.6466
18			.0039	.0859	.3161	.5804
19			.0018	.0565	.2514	.5121
20			.0007	.0358	.1947	.4437
21			.0003	.0217	.1466	.3772
22			.0001	.0127	.1074	.3143
23			.0000	.0071	.0764	.2565
24				.0038	.0528	.2049
25				.0020	.0355	.1602
26				.0010	.0231	.1225
27				.0005	.0146	.0916
28				.0002	.0090	.0673
29				.0001	.0055	.0498
30				.0000	.0041	.0417

Table 25. The concentration function X(z,t) computed for Experiment 2 for Type IV isotherm

Depth	Time (hours)					
	10	20	40	60	80	100
(cm)						
0	1.0000	1.0000	1.0000	1.0000	1.0000	1.0000
1	.8715	.9514	.9863	.9946	.9975	.9967
2	.6890	.8791	.9631	.9847	.9928	.9901
3	.4358	.7874	.9320	.9701	.9852	.9794
4	.1339	.6682	.8946	.9514	.9749	.9644
5	.0119	.5049	.8511	.9294	.9619	.9454
6	.0006	.2834	.8004	.9044	.9468	.9236
7	.0000	.0745	.7393	.8768	.9297	.8998
8		.0088	.6615	.8461	.9111	.8751
9		.0008	.5569	.8117	.8910	.8504
10		.0001	.4108	.7719	.8694	.8259
11		.0000	.2215	.7242	.8459	.8021
12			.0618	.6640	.8202	.7790
13			.0096	.5840	.7913	.7565
14			.0012	.4727	.7580	.7344
15			.0001	.3193	.7182	.7127
16			.0000	.1426	.6683	.6910
17				.0332	.6026	.6688
18				.0053	.5121	.6456
19				.0008	.3850	.6206
20				.0001	.2204	.5928
21				.0000	.0731	.5603
22					.0142	.5203
23					.0023	.4660
24					.0003	.3805
25					.0001	.2315
26					.0000	.0733
27						.0140
28						.0023
29						.0004
30						.0001

Table 26. The concentration function $X(z,t)$ computed for Experiment 2 for Type V isotherm

Depth	Time (hours)					
	10	20	40	60	80	100
(cm)						
0	1.0000	1.0000	1.0000	1.0000	1.0000	1.0000
1	.8470	.9556	.9947	.9993	.9999	1.0000
2	.5814	.8556	.9819	.9977	.9997	1.0000
3	.3668	.6830	.9540	.9940	.9992	.9999
4	.2408	.4987	.8973	.9860	.9982	.9998
5	.1617	.3669	.7962	.9696	.9961	.9995
6	.1080	.2788	.6560	.9368	.9916	.9989
7	.0704	.2164	.5205	.8758	.9827	.9978
8	.0440	.1696	.4185	.7761	.9648	.9955
9	.0260	.1329	.3455	.6492	.9303	.9909
10	.0143	.1036	.2912	.5313	.8684	.9816
11	.0072	.0798	.2489	.4419	.7709	.9635
12	.0033	.0605	.2146	.3766	.6509	.9291
13	.0014	.0449	.1859	.3276	.5410	.8681
14	.0005	.0324	.1614	.2889	.4574	.7734
15	.0002	.0228	.1402	.2573	.3963	.6575
16	.0001	.0154	.1215	.2307	.3503	.5512
17	.0000	.0100	.1050	.2077	.3140	.4702
18		.0063	.0903	.1875	.2844	.4111
19		.0037	.0772	.1695	.2594	.3667
20		.0021	.0655	.1533	.2378	.3320
21		.0011	.0552	.1387	.2187	.3036
22		.0006	.0460	.1253	.2016	.2798
23		.0003	.0379	.1130	.1862	.2592
24		.0001	.0308	.1017	.1722	.2411
25		.0000	.0247	.0912	.1593	.2249
26			.0196	.0816	.1474	.2103
27			.0152	.0729	.1365	.1971
28			.0117	.0650	.1267	.1854
29			.0091	.0587	.1187	.1760
30			.0078	.0555	.1147	.1712

Table 27. The concentration profiles computed by the non-linear method for Experiment 3

Depth	Column 3-I		Column 3-II		Column 3-III	
	X_{Mg}	Y_{Mg}	X_{Mg}	Y_{Mg}	X_{Mg}	Y_{Mg}
(cm)						
0	1.0000	1.0000	1.0000	1.0000	1.0000	1.0000
1	.9929	.9877	.9997	.9994	.9998	.9996
2	.9721	.9533	.9984	.9972	.9991	.9984
3	.9332	.8948	.9952	.9917	.9976	.9958
4	.8757	.8190	.9888	.9807	.9946	.9907
5	.7988	.7329	.9777	.9624	.9896	.9821
6	.6982	.6376	.9613	.9364	.9819	.9692
7	.5637	.5276	.9394	.9037	.9710	.9516
8	.3850	.3906	.9122	.8657	.9569	.9296
9	.1869	.2212	.8797	.8240	.9394	.9036
10	.0571	.0781	.8417	.7792	.9186	.8744
11	.0126	.0183	.7973	.7314	.8947	.8428
12	.0023	.0034	.7448	.6798	.8676	.8093
13	.0004	.0006	.6807	.6224	.8370	.7739
14	.0000	.0001	.5997	.5558	.8026	.7369
15	.0000	.0000	.4941	.4741	.7635	.6977
16			.3580	.3694	.7184	.6556
17			.2051	.2387	.6654	.6095
18			.0850	.1124	.6019	.5575
19			.0270	.0384	.5242	.4971
20			.0074	.0108	.4292	.4247
21			.0019	.0028	.3179	.3371
22			.0004	.0007	.2046	.2382
23			.0001	.0003	.1361	.1697
24			.0000	.0001		
25						

Table 28. The concentration profiles computed by the linear method
for Experiment 3

| Depth | Column 3-I | | Column 3-II | | Column 3-III | |
	X_{Mg}	Y_{Mg}	X_{Mg}	Y_{Mg}	X_{Mg}	Y_{Mg}
(cm)						
0	1.0000	.9600	1.0000	.9600	1.0000	.9600
1	.9976	.9578	.9999	.9599	1.0000	.9600
2	.9887	.9496	.9999	.9599	.9999	.9599
3	.9646	.9274	.9995	.9596	.9998	.9598
4	.9134	.8803	.9987	.9588	.9994	.9595
5	.8247	.7988	.9966	.9568	.9987	.9588
6	.6970	.6812	.9920	.9526	.9973	.9575
7	.5420	.5386	.9831	.9444	.9947	.9551
8	.3827	.3921	.9669	.9295	.9901	.9509
9	.2428	.2634	.9401	.9049	.9825	.9439
10	.1376	.1666	.8991	.8671	.9706	.9329
11	.0692	.1037	.8412	.8139	.9527	.9165
12	.0309	.0684	.7654	.7442	.9273	.8931
13	.0122	.0512	.6737	.6598	.8928	.8614
14	.0043	.0439	.5705	.5649	.8480	.8202
15	.0013	.0412	.4627	.4657	.7926	.7692
16	.0004	.0406	.3580	.3694	.7270	.7089
17	.0001	.0403	.2634	.2824	.6528	.6406
18	.0000	.0401	.1838	.2091	.5725	.5667
19	.0000	.0400	.1214	.1517	.4893	.4902
20	.0000	.0400	.0757	.1097	.4069	.4143
21	.0000	.0400	.0446	.0810	.3291	.3428
22	.0000	.0400	.0247	.0628	.2619	.2809
23	.0000	.0400	.0130	.0520	.2236	.2458
24	.0000	.0400	.0077	.0471		

Table 29. The concentration profiles computed for Experiment 4, Nibley clay loam

Depth	Column 4-I		Column 4-II		Column 4-III	
	X_{Mg}	Y_{Mg}	X_{Mg}	Y_{Mg}	X_{Mg}	Y_{Mg}
(cm)						
0	1.0000	1.0000	1.0000	1.0000	1.0000	1.0000
1	.9123	.7647	.9801	.9313	.9926	.9732
2	.8022	.6080	.9510	.8495	.9799	.9310
3	.6727	.4995	.9160	.7718	.9627	.8802
4	.5169	.4090	.8770	.7039	.9422	.8281
5	.3328	.3116	.8347	.6454	.9194	.7787
6	.1512	.1842	.7886	.5941	.8951	.7334
7	.0418	.0634	.7375	.5476	.8694	.6924
8	.0080	.0131	.6792	.5039	.8425	.6552
9	.0012	.0021	.6108	.4606	.8140	.6209
10	.0002	.0003	.5285	.4150	.7834	.5889
11	.0000	.0001	.4286	.3633	.7501	.5583
12	.0000	.0000	.3110	.2989	.7129	.5282
13			.1877	.2150	.6700	.4977
14			.0873	.1200	.6191	.4655
15			.0314	.0488	.5564	.4300
16			.0096	.0156	.4774	.3885
17			.0026	.0044	.3776	.3364
18			.0007	.0011	.2586	.2662
19			.0002	.0003	.1397	.1737
20			.0000	.0001	.0563	.0826
21			.0000	.0000	.0181	.0290
22					.0062	.0087
23					.0021	.0035
24						
25						

Table 30. The concentration profiles computed for Experiment 4,
Hanford sandy loam

Depth	Column 4-I		Column 4-II		Column 4-III	
	X_{Mg}	Y_{Mg}	X_{Mg}	Y_{Mg}	X_{Mg}	Y_{Mg}
(cm)						
0	1.0000	1.0000	1.0000	1.0000	1.0000	1.0000
1	.9939	.9819	.9999	.9996	1.0000	1.0000
2	.9665	.9095	.9981	.9944	.9999	.9999
3	.9193	.8098	.9910	.9737	1.0000	1.0000
4	.8584	.7120	.9760	.9333	1.0000	1.0000
5	.7821	.6206	.9543	.8810	.9981	.9944
6	.6773	.5268	.9278	.8257	.9920	.9766
7	.5016	.4078	.8978	.7720	.9813	.9471
8	.2119	.2188	.8650	.7213	.9670	.9108
9	.0369	.0489	.8288	.6734	.9505	.8726
10	.0043	.0060	.7881	.6269	.9324	.8349
11	.0004	.0006	.7402	.5797	.9134	.7990
12	.0000	.0001	.6790	.5282	.8936	.7650
13	.0000	.0000	.5893	.4637	.8731	.7331
14			.4317	.3652	.8517	.7028
15			.1859	.1981	.8293	.6739
16			.0381	.0504	.8056	.6460
17			.0066	.0079	.7800	.6184
18			.0008	.0011	.7518	.5905
19			.0001	.0001	.7188	.5607
20			.0000	.0000	.6755	.5254
21			.0000	.0000	.5932	.4663
22					.2813	.2693
23						
24						
25						

Table 31. The concentration profiles computed for Experiment 5 for Yolo fine sandy loam

Depth	Column 5-I		Column 5-II		Column 5-III	
	X_{Na}	Y_{Na}	X_{Na}	Y_{Na}	X_{Na}	Y_{Na}
(cm)						
0	1.0000	1.0000	1.0000	1.0000	1.0000	1.0000
1	.9496	.6191	.9599	.6721	.9751	.7687
2	.8967	.4373	.9138	.4838	.9408	.5798
3	.8497	.3437	.8727	.3843	.9088	.4683
4	.8066	.2852	.8352	.3218	.8794	.3980
5	.7658	.2441	.8000	.2778	.8521	.3475
6	.7263	.2190	.7662	.2445	.8262	.3094
7	.6874	.1880	.7332	.2179	.8013	.2793
8	.6488	.1674	.7004	.1958	.7772	.2545
9	.6109	.1502	.6674	.1769	.7535	.2336
10	.5740	.1356	.6339	.1603	.7300	.2156
11	.5204	.1173	.5994	.1454	.7066	.1997
12	.3260	.0682	.5639	.1319	.6831	.1855
13	.0613	.0143	.5269	.1194	.6593	.1727
14	.0484	.0012	.4839	.1065	.6351	.1608
15	.0000	.0000	.4039	.0857	.6102	.1498
16			.2257	.0478	.5844	.1395
17			.0611	.0143	.5575	.1296
18			.0103	.0025	.5289	.1200
19			.0014	.0003	.4982	.1106
20			.0002	.0000	.4642	.1010
21			.0000	.0000	.4243	.0906
22					.3735	.0786
23						
24						
25						

VITA

Sung-ho Lai

Candidate for the Degree of

Doctor of Philosophy

Dissertation: Cation Exchange and Transport in Soil Column Undergoing
Miscible Displacement

Major Field: Soil Science

Biographical Information:

Personal Data: Born at Miaoli, Taiwan, October 3, 1938; son of
Chiang-tze Lai and Yuh-shiang Shieh Lai; married Sandra Yuk
Hoong Yee December 22, 1968; one child--Alan Hwa-chin Lai.

Education: Degree: Bachelor of Science in Agriculture Chemistry
(National Taiwan University, 1962); Master of Science in Soil
Science (University of Hawaii, 1967); Doctor of Philosophy
(Utah State University, 1971). Scholarship: East-West Center
for Cultural and Technical Interchange, Honolulu, Hawaii, 1964-
1966.

Other Experience: Trainee at U. S. Salinity Laboratory, Riverside,
California, summer 1965; Research Assistant in Soil and
Plant Nutrition Laboratory, National Taiwan University, 1963-
1964; Research Assistant in the Department of Water Science
and Engineering, University of California, Davis, 1967-1968.
Research Assistant, Department of Soils and Meteorology, Utah
State University.

Professional Activities:

Publication: "Chemical Properties of Allophane from Hawaiian
and Japanese Soils." Published in Soil Sci. Soc. Amer. Proc.
33:804-808, 1969.

Papers Presented: "Chemical Properties of Allophane from
Hawaiian and Japanese Soils." Presented at the 59th Annual
Meeting of the Amer. Soc. of Agron., 1967; "Numerical Approxi-
mation of Cation Exchange in Soil Columns Undergoing Miscible
Displacement: Non-linear Exchange Function." Presented at
the 62nd Annual Meeting of the Amer. Soc. of Agron., 1970.

Awards Received: Pacific Division of AAAS Award for Excellence
for paper entitled "Numerical Approximation of Cation Ex-
change in Soil Columns Undergoing Miscible Displacement."
Presented at the 51st Annual Meeting of the Pacific Division
of the American Association for the Advancement of Science,
Berkeley, California, June 21-25, 1970.

Affiliations: American Society of Agronomy; Soil Science Society
of America.